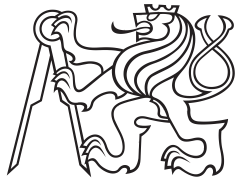


Bachelor Project



Czech
Technical
University
in Prague

F4

Faculty of Nuclear Sciences and Physical Engineering
Department of Physics

Solvable models described by onedimensional Dirac equation and their application in physics of graphene

Petr Červenka

Supervisor: Ing. Vít Jakubský, Ph.D.

Supervisor–specialist: Doc. Ing. Matěj Tušek, Ph.D.

Field of study: Quantum technologies

August 2023

ZADÁNÍ BAKALÁŘSKÉ PRÁCE

Akademický rok: 2022/2023



Student: Petr Červenka

Studijní program: Kvantové technologie

Název práce: Řešitelné modely popsané jednodimenzionální Diracovou rovnicí a jejich aplikace ve fyzice grafénu
(česky)

Název práce: Solvable models described by onedimensional Dirac equation and their application in physics of graphene
(anglicky)

Jazyk práce: Angličtina

Pokyny pro vypracování:

- 1) Seznámení se supersymetrickou kvantovou mechanikou
 - Darbouxova transformace a relace provázání pro Schrodingerův Hamiltonián
 - Darbouxova transformace a relace provázání pro Diracův Hamiltonián
 - transformace řešení mezi provázanými systémy
- 2) Seznámení s popisem Diracovských fermionů v grafénu
 - popis krystalu, Blochův teorém
 - odvození Diracovy rovnice pro fermiony v grafénu
 - efektivní popis interakcí pomocí Diracovy rovnice
- 3) Konstrukce řešitelných modelů popsaných jednodimenzionální Diracovou rovnicí
 - diskuse výhod a úskalí použití Darbouxovy transformace pro konstrukci fyzikálně relevantních systémů, příklady

Doporučená literatura:

- [1] F. Cooper, A. Khare, U. Sukhatme, Supersymmetry in Quantum Mechanics, World Scientific
- [2] G. Junker, Supersymmetric Methods in Quantum and Statistical Physics, Springer 1996
- [3] Nieto, L. M.; Pecheritsin, A. A.; Samsonov, Boris F., Intertwining technique for the one-dimensional stationary Dirac equation, Annals of Physics 305, 151-189 (2003).
- [4] G.W. Semenoff, Condensed-Matter Simulation of a Three-Dimensional Anomaly, Phys. Rev. Lett. 53, 2449-2452 (1984)
- [5] M. Katsnelson, The Physics of Graphene, Cambridge University Press 2020

Jméno a pracoviště vedoucího bakalářské práce:

Ing. Vít Jakubský, Ph.D.

Ústav jaderné fyziky AV ČR, v.v.i., Oddělení teoretické fyziky

Konzultant:


doc. Ing. Matěj Tušek, Ph.D.

Katedra matematiky, Fakulta jaderná a fyzikálně inženýrská ČVUT v Praze

Datum zadání bakalářské práce: 20.10.2022

Termín odevzdání bakalářské práce: 02.08.2023

Doba platnosti zadání je dva roky od data zadání.


.....
garant studijního programu




.....
vedoucí katedry


.....
děkan

V Praze dne 20.10.2022



PROHLÁŠENÍ

Já, níže podepsaný

Jméno a příjmení studenta: Petr Červenka
Osobní číslo: 502680
Název studijního programu (oboru): Kvantové technologie

prohlašuji, že jsem bakalářskou práci s názvem:

**Řešitelné modely popsané jednodimenzionální Diracovou rovnicí
a jejich aplikace ve fyzice grafénu**

vypracoval(a) samostatně a uvedl(a) veškeré použité informační zdroje v souladu s Metodickým pokynem o dodržování etických principů při přípravě vysokoškolských závěrečných prací.

V Praze dne 9. 7. 2023

.....
podpis

Acknowledgements

I would like to express my sincere gratitude to Ing. Vít Jakubský, Ph.D. for his guidance and providing valuable advice and suggestions. I am also thankful to my family for their support during my studies.

Declaration

I hereby declare that the presented thesis is my own work and that I have cited all sources of information in accordance with the Guideline for adhering to ethical principles when elaborating an academic final thesis.

In Prague on 9.7.2023

Abstract

In this work, we investigate various kinds of solvable models for onedimensional Schrödinger and Dirac equation with demonstration on explicit examples. For that purpose, the Darboux transformation is widely used. Using the first quantization tight-binding model, we show the emergence of 2D Dirac equation in the physics of graphene. Strain in graphene nanoribbons and its effect on them is discussed. We reveal the solvability of a certain type of staggered potential in the 2D Dirac equation. The influence of inhomogenous staggered potential on spectral properties of Dirac fermions in the armchair nanoribbons is analyzed.

Keywords: Solvable models, Dirac equation, graphene, nanoribbons

Supervisor: Ing. Vít Jakubský, Ph.D.
Oddělení teoretické fyziky ÚJF AVČR,
Řež 25068

Abstrakt

V této práci prozkoumáme různé typy řešitelných modelů pro jednodimenzionální Schrödingerovu a Diracovu rovnici s demonstrací na konkrétních příkladech. Hojně k tomu budeme používat Darbouxovu transformaci. Pomocí tight-binding modelu v prvním kvantování ukážeme, jak se objeví Diracova rovnice ve fyzice grafénu. Je diskutováno mechanického napětí v grafénových nanoproužcích a jeho efekt na ně. Odhalíme řešitelnost jistého typu staggered potenciálu ve 2D Diracově rovnici. Je analyzován vliv nehomogenního staggered potenciálu na spektrální vlastnosti Diracovských fermionů v armchair nanoproužcích.

Klíčová slova: Řešitelné modely, Diracova rovnice, grafén, nanoproužky

Překlad názvu: Řešitelné modely popsané jednodimenzionální Diracovou rovnicí a jejich aplikace ve fyzice grafénu

Contents

1 Introduction	1	3.2.2 DT of free Dirac particle - example 2	27
2 DT for Schrödinger operator	3	4 Dirac equation in graphene	29
2.1 Factorization of Schrödinger operator	5	4.1 Description of crystals	29
2.2 The approach based on intertwining relations	7	4.2 Bravais lattice and crystal structure	29
2.3 DT of the free particle Hamiltonian	8	4.2.1 Wigner-Seitz cell	30
2.4 DT of infinite square well	10	4.3 Reciprocal lattice	31
2.4.1 Example	12	4.4 Bloch's theorem	32
2.5 DT of finite square well	13	4.5 Tight-binding model graphene . .	33
2.5.1 Regularized $\sec^2(k_0x)$	15	4.6 Interaction in graphene	39
2.5.2 Regularized $\csc^2(kx)$	19	4.6.1 Pseudo-magnetic field	40
2.5.3 Spectra of FSW and its regularized versions	21	4.6.2 Staggered potential	40
3 DT for 1D Dirac operator	23	5 Nanoribbons	43
3.1 Matrix approach of DT	23	5.1 Armchair and zigzag boundary .	44
3.2 DT of free Dirac particle	25	5.2 Projector method	45
3.2.1 DT of free Dirac particle - example 1	26	5.3 Additional constant mass term in Dirac Hamiltonians	46
		5.4 Strained nanoribbons	47

5.5 Formal model of strained nanoribbons.....	48
5.5.1 Strained armchair nanoribbon	50
5.5.2 Strained zigzag nanoribbon..	51
5.6 2D Dirac operator hidden in 1D Dirac operator	52
5.7 AC nanoribbon in staggered field	54
6 Conclusions	59
Bibliography	61



Chapter 1

Introduction

Many fascinating properties of graphene can be described by the 2D Dirac equation, see e.g. [1], [2]. The experimental isolation of graphene has opened the door to its technical applications [3]. It is a promising material which could find attractive usage in many areas of physics [4], [5], [6]. Exactly solvable models are important for the understanding of physics of graphene. They simplify the physical reality, however, they preserve the physical substance of the system and offer analytical solvability. The Dirac equation appears in the low-energy description of quasi-particles in many systems. They are called Dirac materials. The family of Dirac materials does not contain only graphene, but also topological insulators, high-temperature cuprate superconductors or Weyl semimetals [7]. Therefore, solvable models described by 2D or 1D Dirac equation can have broader applicability.

In the thesis, we focus on the construction of such exactly solvable models through the concept of Darboux transformation (DT) related to the supersymmetric quantum mechanics (SUSY QM) [8], [9]. Strength of DT lies in the fact that from the known quantum system we can create the new one whose properties can be derived in a straightforward manner.

The work is organized as follows. In Chapter 2, we present the Darboux transformation for Schrödinger's operator as a mathematical tool for the construction of 1D solvable models. Its application is illustrated on the examples of the models infinite (ISW) and finite square wells (FSW). Chapter 3 is dedicated to the generalization of DT for the 1D Dirac operator [10]. Explicit examples are discussed where the transformation is applied on the model of 1D free Dirac particle. The connection between the physics of graphene and the Dirac equation comes from the tight-binding model, which is presented in Chapter 4 [11], [12]. Here, we also outline the effective interactions in graphene [13], [14]. The main effort has been concentrated to Chapter 5 that is dedicated to nanoribbons. It begins with the description of zigzag (ZZ) and armchair (AC) edges [15], [16], [17]. Then we move on to

an extension of the 1D Dirac equation to two dimensions. Finally, two physically relevant models of strained and staggered nanoribbons are the highlights of the chapter.

Chapter 2

DT for Schrödinger operator

Supersymmetry, the symmetry between particles with integer and half-integer spin, caused a stir in physics. SUSY is based on the idea that every fermion has a bosonic superpartner and the other way round. In the beginning, it was used in the quantum field theory. In particle physics, it was believed to explain the origin of dark matter or to unify weak, strong and electromagnetic forces. Nevertheless, its experimental confirmation is still to come. SUSY in the quantum field theory stems on the superalgebra of the involved operators. In [18], [19], Nicolai and Witten introduced a toy model of supersymmetric quantum system that preserved the superalgebraic structure of the operators. This way, the supersymmetry found its way to QM. It founded an independent field of research named supersymmetric quantum mechanics. It was based on the factorization of Schrödinger Hamiltonians similar to the formalism of ladder operators. It is worth mentioning that the same manipulation of differential equations was proposed by Darboux [20]. These Darboux's results were brushed up and they were further broadened [21]. The concepts of SUSY QM are summarized in [8], [9].

Quantum system is supersymmetric whenever the operators Q_1, Q_2, \dots, Q_N, H , that characterize the system, satisfy [9]

$$\{Q_i, Q_j\} = \delta_{ij}H. \quad (2.1)$$

We are interested in $N = 2$ SUSY QM which means the existence of two self-adjoint operators Q_1, Q_2 , *supercharges*. We define the complex supercharges $Q = \frac{1}{\sqrt{2}}(Q_1 + iQ_2)$, $Q^\dagger = \frac{1}{\sqrt{2}}(Q_1 - iQ_2)$. Together with H , they obey the superalgebra

$$H = \{Q, Q^\dagger\}, \quad Q^2 = 0, \quad (Q^\dagger)^2 = 0. \quad (2.2)$$

The energy of a quantum system with the Hamiltonian, which appears in the superalgebra, is always $\langle \psi | H | \psi \rangle = \|Q\psi\|^2 + \|Q^\dagger\psi\|^2 \geq 0$. Therefore, there must exist a state with the minimal energy E_0 alias the ground state $|\psi_0\rangle$. In the case of $E_0 = 0$, both supercharges Q, Q^\dagger annihilate $|\psi_0\rangle$, i.e. $Q|\psi_0\rangle = Q^\dagger|\psi_0\rangle = 0$. When $E_0 = 0$ then SUSY is a *good symmetry*, otherwise SUSY is a *broken symmetry*. Due to $[H, Q] = [H, Q^\dagger] = 0$, the action of supercharges is closed in the subspaces for energy E . Indeed, $HQ|\psi\rangle = QH|\psi\rangle = EQ|\psi\rangle$. Relations (2.2) also imply $Q^2|\psi\rangle = (Q^\dagger)^2|\psi\rangle = 0$. In the subspace of fixed E , we can define the operators

$$b^\dagger = \frac{Q}{\sqrt{E}}, \quad b = \frac{Q^\dagger}{\sqrt{E}}, \quad \{b, b^\dagger\} = 1, \quad \{b, b\} = \{b^\dagger, b^\dagger\} = 0. \quad (2.3)$$

We see that they satisfy fermionic anticommutation relations. As we know, there exist only fermionic states $|0\rangle, |1\rangle$. We can introduce the fermion number operator F ,

$$F = b^\dagger b, \quad F|0\rangle = 0, \quad F|1\rangle = |1\rangle. \quad (2.4)$$

With this knowledge, we can construct the Witten parity operator $\hat{W} = 2F - 1$ and orthogonal projectors $P_\pm = \frac{1}{2}(1 \pm \hat{W}) = \frac{1}{2}(1 \pm 2F \mp 1)$. Apparently, $P_-|0\rangle = |0\rangle, P_+|0\rangle = 0, P_+|1\rangle = |1\rangle, P_-|1\rangle = 0$. They decompose the Hilbert space into

$$\mathcal{H} = \mathcal{H}_+ \oplus \mathcal{H}_-, \quad P_+\mathcal{H} = \mathcal{H}_+, \quad P_-\mathcal{H} = \mathcal{H}_-. \quad (2.5)$$

If we represent $\psi_+(x) = \langle x|1\rangle = (0, \phi_+(x))^T \in \mathcal{H}_+, \psi_-(x) = \langle x|0\rangle = (\phi_-(x), 0)^T \in \mathcal{H}_-$, we can write the operators Q, Q^\dagger, H, \hat{W} in the matrix form. From $Q^2 = 0, \{Q, \hat{W}\} = 0$, it follows that Q, \hat{W} have the only possible form

$$Q = \begin{pmatrix} 0 & \hat{A} \\ 0 & 0 \end{pmatrix}, \quad Q^\dagger = \begin{pmatrix} 0 & 0 \\ \hat{A}^\dagger & 0 \end{pmatrix}, \quad \hat{W} = \begin{pmatrix} 1 & 0 \\ 0 & -1 \end{pmatrix}. \quad (2.6)$$

The Hamiltonian is given by (2.2). It is in the diagonal form

$$H = \{Q, Q^\dagger\} = \begin{pmatrix} \hat{A}\hat{A}^\dagger & 0 \\ 0 & \hat{A}^\dagger\hat{A} \end{pmatrix}. \quad (2.7)$$

Due to $[\hat{W}, H] = 0$, the Hamiltonian H and the parity operator \hat{W} have common eigenstates. We denote them as $\psi_{E+} \equiv \psi_+, \psi_{E-} \equiv \psi_-$ where $H\psi_{E\pm} = E\psi_{E\pm}$ and $\hat{W}\psi_{E\pm} = \pm\psi_{E\pm}$. Between \mathcal{H}_+ and \mathcal{H}_- , there is a mapping via $b \propto Q^\dagger$ and $b^\dagger \propto Q$. In fact, $Q^\dagger|1\rangle \propto \langle b|1\rangle = |0\rangle \in \mathcal{H}_-$ and $Q|0\rangle \propto \langle b^\dagger|0\rangle = |1\rangle \in \mathcal{H}_+$. For a fixed positive energy, normalized eigenfunctions can be rewritten as

$$\begin{aligned} \psi_{E+}(x) &= \frac{Q\psi_{E-}(x)}{\sqrt{E}}, & \psi_{E-}(x) &= \frac{Q^\dagger\psi_{E+}(x)}{\sqrt{E}}, \\ \phi_{E+}(x) &= \frac{\hat{A}\phi_{E-}(x)}{\sqrt{E}}, & \phi_{E-}(x) &= \frac{\hat{A}^\dagger\phi_{E+}(x)}{\sqrt{E}}. \end{aligned} \quad (2.8)$$

The eigenstate ψ_{E-} of H implies that ϕ_{E-} is the eigenstate of $\hat{A}^\dagger \hat{A}$ with the eigenvalue E . Using Q , we construct the eigenstate $\psi_{E+}(x) = \frac{Q\psi_{E-}(x)}{\sqrt{E}}$ of H . Then $\phi_{E+} = \frac{\hat{A}\psi_{E-}(x)}{\sqrt{E}}$ is the eigenstate of $\hat{A}\hat{A}^\dagger$ with the eigenvalue E . Thus, the spectra of $\hat{A}\hat{A}^\dagger$ and $\hat{A}^\dagger\hat{A}$ coincide for $E > 0$. The energy level $E = 0$ is an exception. It can be present in the spectrum of $\hat{A}^\dagger\hat{A}$ while missing in the spectrum of $\hat{A}\hat{A}^\dagger$ and vice versa. In the Witten formulation of $N = 2$ SUSY, there holds true

$$\begin{aligned} \text{good SUSY : } & \sigma(\hat{A}^\dagger\hat{A}) \setminus \{0\} = \sigma(\hat{A}\hat{A}^\dagger) \\ \text{broken SUSY : } & \sigma(\hat{A}^\dagger\hat{A}) = \sigma(\hat{A}\hat{A}^\dagger). \end{aligned} \quad (2.9)$$

2.1 Factorization of Schrödinger operator

Let us assume a quantum system which is described by the one-dimensional time-independent Hamiltonian H_1

$$H_1 = -\partial_x^2 + V_1, \quad (2.10)$$

where V_1 is required to be a real-valued function. We will assume that H_1 is self-adjoint, i.e. $H_1 = H_1^\dagger$. Our goal is to factorize H_1 in terms of differential operators \hat{A} , \hat{A}^\dagger

$$H_1 - E_0 = \hat{A}^\dagger \hat{A}, \quad (2.11)$$

where $E_0 \in \mathbb{R}$. The parameter E_0 has to be real, since the right-hand side of (2.11) is a Hermitian operator, $(\hat{A}^\dagger \hat{A})^\dagger = \hat{A}^\dagger \hat{A}$. The Hamiltonian H_1 is a second-order differential operator. Thus, \hat{A} should be taken as a first-order differential operator ($\hat{A}^\dagger \hat{A}$ is then second-order). We make an ansatz

$$\hat{A} = f \partial_x \frac{1}{f} = \partial_x + W, \quad \hat{A}^\dagger = -\frac{1}{f} \partial_x f = -\partial_x + W, \quad W = -\frac{f'}{f}. \quad (2.12)$$

$\hat{A}f = f \partial_x \frac{f}{f} = 0$, so $f \in \ker(\hat{A})$. The function f has to be fixed such that (2.11) is satisfied.

We have

$$\hat{A}^\dagger \hat{A} = [f^{-1}(-\partial_x)f] [f \partial_x f^{-1}] = \left(-\partial_x - \frac{f'}{f}\right) \left(\partial_x - \frac{f'}{f}\right) = -\partial_x^2 + \frac{f''}{f}. \quad (2.13)$$

Substituting (2.13) into (2.11), we get

$$H_1 - E_0 = -\partial_x^2 + \frac{f''}{f}. \quad (2.14)$$

It implies that the function f must be a solution of

$$-f'' + V_1 f = E_0 f. \quad (2.15)$$

It is obvious that it is the same as $H_1 f = E_0 f$. Thus, the factorization (2.11) of H_1 can be made in terms of operators (2.12), where f is an eigenstate of H_1 corresponding to the eigenvalue E_0 .

Now, let us define a new operator H_2 as follows,

$$\begin{aligned} H_2 - E_0 &\equiv \hat{A}\hat{A}^\dagger = [f\partial_x f^{-1}] [f^{-1}(-\partial_x)f] = -\partial_x^2 - \frac{f''}{f} + 2\left(\frac{f'}{f}\right)^2 = \\ &= -\partial_x^2 + V_1 - 2(\ln(f))'' - E_0 = -\partial_x^2 + V_2 - E_0. \end{aligned} \quad (2.16)$$

The operator is Hermitian by construction. It has the structure of Schrödinger's operator. Therefore, $H_2 - E_0 = -\partial_x^2 + V_2 - E_0 = \hat{A}\hat{A}^\dagger$ can serve as a Hamiltonian for the new quantum system. The factorization of $H_1 - E_0 = \hat{A}^\dagger\hat{A}$ and $H_2 - E_0 = \hat{A}\hat{A}^\dagger$ allows us to write down the following relations

$$\hat{A}H_1 = H_2\hat{A}, \quad (2.17)$$

$$H_1\hat{A}^\dagger = \hat{A}^\dagger H_2. \quad (2.18)$$

We can see that H_1 and H_2 are intertwined by the operator \hat{A} . The eqs. (2.17) and (2.18) are called the *intertwining relations*. The relations (2.12) and (2.16) tell us that for any f satisfying (2.15), we can construct the new Hamiltonian H_2 and the operator \hat{A} such that (2.17) holds. The function f is named the *seed solution*. Witten also set the ansatz $\hat{A} = \partial_x + W(x)$ in his study of $N = 2$ supersymmetric quantum systems [19], [9].

The factorization procedure has important consequences. Let us assume that $H_1\psi = E\psi$ is solvable for any $E \in \mathbb{R}$. The stationary equation $H_2\phi = E\phi$ can be easily solved. Indeed, the intertwining relation (2.17) allow us to transform the known eigenstates ψ of H_1 to the eigenstates of H_2 as follows

$$H_2(\hat{A}\psi) = \hat{A}\hat{A}^\dagger\hat{A}\psi = \hat{A}H_1\psi = E\hat{A}\psi. \quad (2.19)$$

Therefore, $\hat{A}\psi$ is the eigenstate of H_2 with the energy E . We emphasize that $\hat{A}\psi$ may or may not be a physical state. It must be checked whether $\hat{A}\psi$ complies with the boundary conditions (b.c.) prescribed for the eigenstates of H_2 . The transformation does not guarantee their automatic fulfillment.

The other property of factorization is that we can create a new solvable potential V_2 . It is obtained by the comparison of $-\partial_x^2 + V_2 - E_0 = H_2 - E_0 = \hat{A}\hat{A}^\dagger$

$$V_2 = V_1 - 2(\ln f)'' = W' + W^2 + E_0. \quad (2.20)$$

From the form of (2.20), we can see that real-valued f and V_1 guarantee real-valued V_2 . Furthermore, V_2 can differ dramatically from V_1 . If f had zeros, the potential V_2 would be singular. In that case, the corresponding b.c. must be specified in the singularities of V_2 .

2.2 The approach based on intertwining relations

Let us consider an alternative approach to the construction of H_1 and H_2 that is centred on the intertwining relation (2.17) from the very beginning. Let us suppose that H_1 is known. We assume that $H_2 = -\partial_x^2 + V_2(x)$ where V_2 is to be fixed. We make an ansatz for the operator \hat{A} as

$$\hat{A} = C_1(x)\partial_x + C_2(x), \quad C_1, C_2 : \mathbb{R} \mapsto \mathbb{C}. \quad (2.21)$$

We have chosen the first-order differential operator. We could have taken the second-, third-, or higher-order differential operator. We substitute the operator \hat{A} into the intertwining relation (2.17) and we get

$$(C_1\partial_x + C_2)(-\partial_x^2 + V_1) = (-\partial_x^2 + V_2)(C_1\partial_x + C_2). \quad (2.22)$$

By comparing coefficients at the derivatives, we come to

$$\begin{aligned} \partial_x^2 : -2C_1' &= 0 \\ \partial_x^1 : C_1V_1 &= -C_1'' - 2C_2' + V_2C_1 \\ \partial_x^0 : C_2V_1 + C_1V_1' &= -C_2'' + V_2C_2. \end{aligned} \quad (2.23)$$

From the first equation, we see $C_1 = \text{const}$. It can be taken as $C_1 = 1$ (otherwise, we divide the equations by C_1 and redefine $\tilde{C}_2 = \frac{C_2}{C_1}$). The equations (2.23) are reduced to

$$\begin{aligned} \partial_x^1 : V_1 &= -2C_2' + V_2 \\ \partial_x^0 : C_2V_1 + V_1' &= -C_2'' + V_2C_2. \end{aligned} \quad (2.24)$$

Eliminating V_2 from the second equation, we obtain

$$C_2'' - 2C_2C_2' + V_1' = 0. \quad (2.25)$$

It can be expressed as

$$[C_2' - C_2^2 + V_1]' = 0. \quad (2.26)$$

After the integration, we obtain the Riccati equation

$$C_2' - C_2^2 + V_1 = E_0, \quad E_0 \in \mathbb{C}. \quad (2.27)$$

We can linearize the Riccati equation by $C_2 = -\frac{f'}{f}$, $f : \mathbb{R} \mapsto \mathbb{C}$

$$-\frac{f''}{f} + V_1 = E_0. \quad (2.28)$$

The final form is

$$-\frac{f''}{f} + V_1 = E_0, \quad E_0 \in \mathbb{C}. \quad (2.29)$$

It says that f must be an eigenstate of H_1 for the energy E_0 . With this knowledge, we are able to assemble the intertwining operator \hat{A}

$$\hat{A} = \partial_x - \frac{f'}{f} = \partial_x + W. \quad (2.30)$$

From the first equation of (2.24), we calculate

$$V_2 = V_1 - 2 \left(\frac{f'}{f} \right)' = V_1 - 2(\ln f)'' = W' + W^2 + E_0. \quad (2.31)$$

In the previous section, we factorized $H_1 - E_0 = \hat{A}^\dagger \hat{A}$. The hermiticity of $\hat{A}^\dagger \hat{A}$ was implied by $E_0 \in \mathbb{R}$. On the contrary, E_0 can be complex-valued now, see (2.29). The advantages of this approach are multiple. First, it can be applied on H_1 , which is the first-order operator, as we will see later. Second, \hat{A}^\dagger is not needed. Therefore, $W = -\frac{f'}{f}$ can be complex-valued in general. When W is complex-valued, then V_2 can become a complex-valued potential. Schrödinger operators with complex-valued potentials appear in the description of PT-symmetric optical systems [22].

2.3 DT of the free particle Hamiltonian

The free particle (FP) model can serve as a possible starting point for creating new systems. The Schrödinger equation for the free particle reads as

$$-\psi'' = E\psi. \quad (2.32)$$

The general solution can be found in a straightforward manner as

$$\psi(x) = Ae^{ikx} + Be^{-ikx}, \quad A, B \in \mathbb{C}, \quad k = \pm\sqrt{E}. \quad (2.33)$$

We select an eigenstate $\psi_0 = C_1 e^{ik_0 x} + C_2 e^{-ik_0 x}$ with the corresponding eigenvalue $E_0 = k_0^2$ and we construct

$$W = -\frac{\psi_0'}{\psi_0} = -ik_0 \frac{C_1 e^{ik_0 x} - C_2 e^{-ik_0 x}}{C_1 e^{ik_0 x} + C_2 e^{-ik_0 x}}. \quad (2.34)$$

The new potential is given by (2.31)

$$V_2 = W' + W^2 + E_0. \quad (2.35)$$

It has the following explicit form

$$V_2 = 2k_0^2 \left[1 - \left(\frac{C_1 e^{ik_0 x} - C_2 e^{-ik_0 x}}{C_1 e^{ik_0 x} + C_2 e^{-ik_0 x}} \right)^2 \right] = 2k_0^2 \left[1 - \left(\frac{C_1 e^{ik_0 x} - C_2 e^{-ik_0 x}}{\psi_0(x)} \right)^2 \right]. \quad (2.36)$$

Applying the operator $\hat{A} = \partial_x + W$ on a generic wavefunction (2.33), we get

$$\hat{A}\psi = (\partial_x + W)\psi = ik(Ae^{ikx} - Be^{-ikx}) - ik_0 \frac{C_1 e^{ik_0 x} - C_2 e^{-ik_0 x}}{C_1 e^{ik_0 x} + C_2 e^{-ik_0 x}} (Ae^{ikx} + Be^{-ikx}). \quad (2.37)$$

By construction, $\hat{A}\psi$ is the eigenstate of $H_2 = -\partial_x^2 + V_2$. Below, we discuss the properties of V_2 .

We want $V_2(x) \in \mathbb{R}$. Hermiticity of V_2 will be granted provided that (see (2.36))

$$\frac{C_1 e^{ik_0 x} - C_2 e^{-ik_0 x}}{C_1 e^{ik_0 x} + C_2 e^{-ik_0 x}} \in \mathbb{R} \quad \vee \quad i \frac{C_1 e^{ik_0 x} - C_2 e^{-ik_0 x}}{C_1 e^{ik_0 x} + C_2 e^{-ik_0 x}} \in \mathbb{R}. \quad (2.38)$$

It is equivalent to $W \in \mathbb{R}$ or $W \in i\mathbb{R}$. Let us subtract the real and imaginary parts of (2.38). We get

$$\frac{C_1 e^{ik_0 x} - C_2 e^{-ik_0 x}}{C_1 e^{ik_0 x} + C_2 e^{-ik_0 x}} = \frac{|C_1|^2 - |C_2|^2 + \overline{C_2} C_1 e^{2ik_0 x} - \overline{C_1} C_2 e^{-2ik_0 x}}{|C_1|^2 + |C_2|^2 + \overline{C_2} C_1 e^{2ik_0 x} + \overline{C_1} C_2 e^{-2ik_0 x}}. \quad (2.39)$$

In this expression, the denominator is real. The complex part of the numerator is $\overline{C_2} C_1 e^{2ik_0 x} - \overline{C_1} C_2 e^{-2ik_0 x}$. By choice

$$|C_1| = |C_2|, \quad (2.40)$$

the numerator becomes purely imaginary. Thus, we satisfy (2.38). The cancellation of imaginary part of (2.39) is the other option for keeping V_2 real

$$\text{Im}\{\overline{C_2} C_1 e^{2ik_0 x} - \overline{C_1} C_2 e^{-2ik_0 x}\} = 2 \text{Im}\{\overline{C_2} C_1 e^{2ik_0 x}\} = 0. \quad (2.41)$$

The simple choice to satisfy (2.41) would be $(C_1 = 0 \vee C_2 = 0)$. But then the exponentials in (2.36) cancel out and V_2 reduces to a constant. Such a choice would bring us back to the free particle. Thus, we look at the condition

$$\overline{C_2} C_1 e^{2ik_0 x} \in \mathbb{R} \setminus \{0\} \quad (2.42)$$

which gives the restrictions on C_1, C_2 . Coefficients $C_1 = a + ib, C_2 = c + id$ ($a, b, c, d \in \mathbb{R}$) must satisfy

$$(c - id)(a + ib)e^{2i\sqrt{E_0}x} \in \mathbb{R}. \quad (2.43)$$

The exponential can be real ($E_0 < 0$) or complex-valued ($E_0 \geq 0$). For complex-valued exponentials, one of the coefficients must be zero, precisely $C_1 \overline{C_2} = 0$, which we have already excluded. For the real-valued exponential we set $C_1 \overline{C_2} \in \mathbb{R}$.

We come to the conclusion that the potential V_2 in (2.36) is real-valued only when

1. $|C_1| = |C_2|, E_0 \in \mathbb{R}$,
2. $C_1 \overline{C_2} \in \mathbb{R}, E_0 < 0$.

From (2.36), it is evident that V_2 has singularities in the points ξ , where $\psi_0(\xi) = 0$

$$\psi_0(\xi) = C_1 e^{ik_0 \xi} + C_2 e^{-ik_0 \xi} = 0. \quad (2.44)$$

The fact will be useful further in the text.

2.4 DT of infinite square well

The particle in an infinite potential square well (ISW) problem is well known. Its spectrum and eigenfunctions are

$$\begin{aligned} \psi_0 &= C_1 \cos(kx), & k &= \frac{(n + \frac{1}{2})\pi}{L}, & n &= 0, 1, 2, \dots \\ \psi_0 &= C_2 \sin(kx), & k &= \frac{n\pi}{L}, & n &= 1, 2, 3, \dots, \end{aligned} \quad (2.45)$$

for $x \in [-L, L]$, $k = \sqrt{E}$, $E > 0$, $L > 0$. The boundary conditions (b.c.) are $\psi_0(\pm L) = 0$.

We will analyze the DT of a free particle model. From the beginning, we will require the eigenstates of a transformed system to be compatible with the Dirichlet b.c. in $\pm L$. We start with a seed solution ψ_0 given by (2.33) which solves the FP problem. The seed solution generates \hat{A} and W given by (2.12). It vanishes in a set of points $\xi \in \{x_i, \pm L\} \subset [-L, L]$, i.e. $\psi_0(\xi) = 0$. It follows from (2.36) that ξ are singular points of V_2 .

The function to be transformed is again the FP eigenstate, we denote it ψ , $\psi \neq \psi_0$. Transformed functions are $\hat{A}\psi$. For them, we prescribe Dirichlet b.c. in $\pm L$ and in the singular points x_i of V_2 . So, they have to satisfy

$$\lim_{x \rightarrow \xi} (\hat{A}\psi)(x) = 0, \quad \xi \in \{x_i, \pm L\}. \quad (2.46)$$

Afterwards, we would like to specify how to select such ψ that matches the b.c. For that, it is necessary to

$$0 = \lim_{x \rightarrow \xi} \hat{A}\psi(x) = \lim_{x \rightarrow \xi} \left[\psi'(x) - \frac{\psi_0'(x)}{\psi_0(x)} \psi(x) \right], \quad \forall \xi \in \{x_i, \pm L\}. \quad (2.47)$$

If we take a look at the form of ψ_0 in (2.33) then when $\psi_0(\xi) = 0$ subsequently $\psi_0'(\xi) \neq 0$. Inevitably, the function ψ must compensate zeros of ψ_0 . Otherwise, $\hat{A}\psi(x)$ diverges in ξ . It implies the following condition for $\psi(x)$

$$\psi_0(x) \xrightarrow{x \rightarrow \xi} 0 \implies \psi(x) \xrightarrow{x \rightarrow \xi} 0. \quad (2.48)$$

If we choose ψ that fits the above implication, it is the best of both worlds. The limit (2.47) is always equal to zero. It can be shown from the explicit forms of ψ , ψ_0 , $\psi_0(\xi) = \psi(\xi) = 0$

and with L'Hospital's rule. We come to the conclusion that when (2.48) is valid, then (2.47) is automatically fulfilled. It also provides an instruction on how to find ψ , such that $\hat{A}\psi$ satisfies all b.c. in (2.46). The zeros of ψ_0 must be a subset of the zeros of ψ . Thanks to the oscillation theorem¹, ψ must be a state with a higher energy than the seed solution, i.e. $k^2 = E > E_0 = k_0^2$.

Now, let us suppose that $(\forall x \in [-L, L]) (\psi_0(x) \neq 0)$. Transformed solutions must still obey $(\hat{A}\psi)(\pm L) = 0$. Substituting the general solution for the free particle (2.37) to $\hat{A}\psi(\pm L) = 0$, we have two equations

$$\begin{aligned} 0 &= \hat{A}\psi(L) = ik(Ae^{ikL} - Be^{-ikL}) - ik_0 \frac{C_1 e^{ik_0 L} - C_2 e^{-ik_0 L}}{C_1 e^{ik_0 L} + C_2 e^{-ik_0 L}} (Ae^{ikL} + Be^{-ikL}) \\ 0 &= \hat{A}\psi(-L) = ik(Ae^{-ikL} - Be^{ikL}) - ik_0 \frac{C_1 e^{-ik_0 L} - C_2 e^{ik_0 L}}{C_1 e^{-ik_0 L} + C_2 e^{ik_0 L}} (Ae^{-ikL} + Be^{ikL}) \end{aligned} \quad (2.49)$$

for the unknowns A, B, k . It can be rewritten to the form

$$\begin{aligned} Ae^{ikL} \left(k - k_0 \frac{C_1 e^{ik_0 L} - C_2 e^{-ik_0 L}}{C_1 e^{ik_0 L} + C_2 e^{-ik_0 L}} \right) - Be^{-ikL} \left(k + k_0 \frac{C_1 e^{ik_0 L} - C_2 e^{-ik_0 L}}{C_1 e^{ik_0 L} + C_2 e^{-ik_0 L}} \right) &= 0 \\ Ae^{-ikL} \left(k - k_0 \frac{C_1 e^{-ik_0 L} - C_2 e^{ik_0 L}}{C_1 e^{-ik_0 L} + C_2 e^{ik_0 L}} \right) - Be^{ikL} \left(k + k_0 \frac{C_1 e^{-ik_0 L} - C_2 e^{ik_0 L}}{C_1 e^{-ik_0 L} + C_2 e^{ik_0 L}} \right) &= 0. \end{aligned} \quad (2.50)$$

We look for a non-trivial solution, i.e. $(A, B) \neq (0, 0)$. We have to set the determinant equal to zero. The simplification of the determinant is strictly algebraic. The result is the following equation for $k = \sqrt{E}$

$$\begin{aligned} 0 &= 4C_1 C_2 k k_0 \cos(2kL) \sin(2k_0 L) + \\ &+ \left[k^2(C_1^2 + C_2^2 + 2C_1 C_2 \cos(2k_0 L)) - k_0^2(C_1^2 + C_2^2 - 2C_1 C_2 \cos(2k_0 L)) \right] \sin(2kL). \end{aligned} \quad (2.51)$$

There are mixed imaginary and real parts, because C_1, C_2, k can be complex-valued. The parameter k appears in sine, cosine and out of them. In the worst case, we would obtain two (for the real and imaginary parts) transcendental equations. Both must be solved numerically, which is a demanding task. Bypassing this horror, one solution of (2.51) is immediately visible, it is

$$\sin(2k_0 L) = 0 \wedge \sin(2kL) = 0. \quad (2.52)$$

By choice $k = \frac{n\pi}{2L}$, $k_0 = \frac{n_0\pi}{2L}$; $n, n_0 \in \mathbb{N}$ we satisfy $\sin(2k_0 L) = \sin(2kL) = 0$. Compared to (2.45), we see that $k_0 = \sqrt{E_0} = \frac{n_0\pi}{2L}$ and $k = \sqrt{E} = \frac{n\pi}{2L}$ are energies of the infinite

¹The Schrödinger operator $-\partial_x^2$ is also the Sturm-Liouville (S-L) operator. For the eigenvalue equation $-\psi'' = \lambda\psi$ with b.c. $\psi(a) = \psi(b) = 0$, the S-L theory implies [23]:

1. When $\lambda \leq 0$ then all solutions are $\psi \equiv 0$.
2. The spectrum of $-\partial_x^2$ is discrete. Lambdas can be labeled such that $\lambda_0 < \lambda_1 < \dots$
3. The eigenfunctions of $-\partial_x^2$ form an orthogonal set in $L^2([a, b])$. They can be labeled $\{\psi_n\}_{n=0}^{+\infty}$ in such a way that ψ_0 has the eigenvalue λ_0 and so on.
4. The eigenfunction ψ_n has n zeros in (a, b) .
5. At least one zero of ψ_m is between two zeros of ψ_n ($m > n$) in $[a, b]$.

square well. However, the ISW eigenstates always vanish in $\pm L$. In the very beginning, we assumed $\psi_0(\pm L) \neq 0$. So, we cannot set $\sin(k_0L) = \sin(kL) = 0$ and we have to find another solution of (2.51). Nevertheless, it is complicated and we abandon it.

The output is observation (2.48) that if ψ_0 has zero points $\xi \in \{x_i, \pm L\} \subset [-L, L]$ then $\hat{A}\psi(\xi) = 0$ provided that $\psi(\xi) = 0$. This is possible by choosing ψ_0, ψ as solutions of the ISW, see (2.45).

2.4.1 Example

First, we begin with the seed solution

$$\psi_0(x) = \sin(k_0L) = \sin\left(\frac{n_0\pi}{L}x\right), \quad n_0 \in \mathbb{N}. \quad (2.53)$$

The superpotential W and the intertwining operator \hat{A} have the form

$$W(x) = -\frac{\psi_0'(x)}{\psi_0(x)} = -k_0 \cotg(k_0x), \quad \hat{A} = \partial_x + W. \quad (2.54)$$

The new potential V_2 is given by (2.20). Its explicit form is

$$V_2(x) = \frac{2k_0^2}{\sin^2(k_0x)}. \quad (2.55)$$

The singularities of V_2 are the zeros of $\sin(k_0x)$ in the interval $[-L, L]$. That is, points $\xi \in M \equiv \left\{-\frac{n_0}{n_0}L, -\frac{n_0-1}{n_0}L, \dots, \frac{n_0-1}{n_0}L, \frac{n_0}{n_0}L\right\}$. We want to find the eigenstates of $H_2\phi = E\phi$ that comply with b.c. in (2.46). From the DT we can set $\phi = \hat{A}\psi$, where

$$\begin{aligned} \hat{A}\psi &= k[-A\sin(kx) + B\cos(kx)] - k_0 \cotg(k_0x)[A\cos(kx) + B\sin(kx)], \\ \psi &= A\cos(kx) + B\sin(kx), \quad A, B \in \mathbb{R}. \end{aligned} \quad (2.56)$$

According to (2.48), there must equivalently hold $\psi(\xi) = 0, \forall \xi \in M$. Due to $0 \in M$, we fix $A = 0$ in (2.56). After that, ψ is reduced to $\psi(x) = B\sin(kx)$. We have to solve $\forall \xi \in M, \psi(\xi) = 0$, which can be rewritten as

$$(\forall m \in \{-n_0, -n_0+1, \dots, n_0\}) \left(\psi\left(\frac{m}{n_0}L\right) = B\sin\left(k\frac{m}{n_0}L\right) = 0 \right). \quad (2.57)$$

It implies that the zeros of ψ have to be in the same positions as the zeros of ψ_0 . Of course, ψ can have more zeros than ψ_0 , but not less. Thus, ψ is a higher excitation than the seed solution ψ_0 ($k > k_0$). One can check that

$$k = \frac{n_0s\pi}{L}, \quad s \in \mathbb{N} \quad (2.58)$$

satisfies $\psi(\xi) = B\sin(k\xi) = 0, \forall \xi \in M$. We can skip $s = 1$, because then $k = k_0$ is the seed solution state, which is annihilated by \hat{A} .

Owing to $E = k^2$, we obtain the energy spectrum and eigenfunctions of the Hamiltonian $H_2 = -\partial_x^2 + V_2$ as

$$E = k^2 = \left(\frac{n_0 s \pi}{L}\right)^2; \quad n_0 \in \mathbb{N}, \quad s \in \{2, 3, 4, \dots\},$$

$$\hat{A}\psi = \frac{n_0 s \pi}{L} B \cos\left(\frac{n_0 s \pi}{L} x\right) - B \frac{n_0 \pi}{L} \cotg\left(\frac{n_0 \pi}{L} x\right) \sin\left(\frac{n_0 s \pi}{L} x\right).$$
(2.59)

Always $\sqrt{E} = k > k_0 = \sqrt{E_0}$, therefore energies smaller than E_0 are missing in the transformed system. The higher excited state ψ_0 (higher n_0) implies that the gaps between two energy levels in the transformed system are larger. For $n_0 = 2$, the wavefunctions (2.59) are shown in Fig. 2.1.

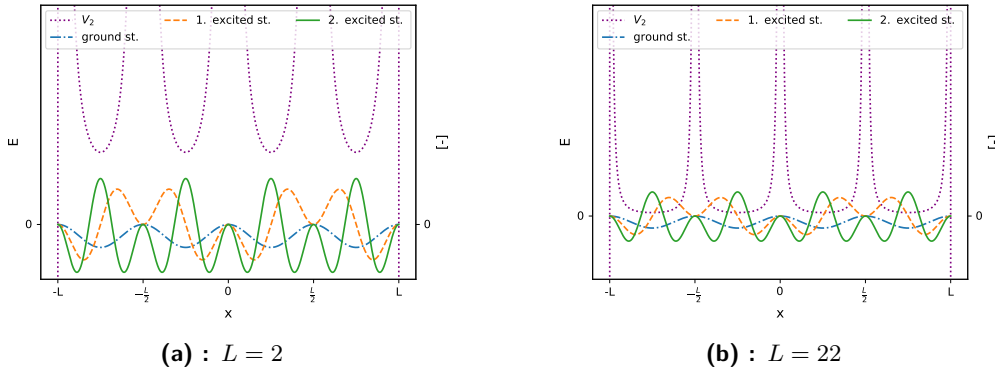


Figure 2.1: The potential $V_2(x)$ given by (2.55) with different L . We denote the ground state as ψ_2 , the 1st excited state as ψ_3 and the 2nd excited state as ψ_4 . The eigenfunctions are then $\psi_n = k_n B \cos(k_n x) - \frac{2\pi}{L} \cotg\left(\frac{2\pi}{L} x\right) B \sin(k_n x)$ with $k_n = n \frac{2\pi}{L}$ for $n = 2, 3, 4$. The wavefunctions can vanish in three wells and be non-zero in one well. These states are orthogonal, they are still the eigenstates of H_2 with the eigenvalue E_n and we speak about the fourfold degeneracy.

2.5 DT of finite square well

We will apply the Darboux transformation to the model of a finite square well (FSW). We start with the step potential for the FSW

$$V_1(x) = \begin{cases} V_0, & x < -L \\ 0, & |x| \leq L \\ V_0, & x > L \end{cases} \quad (2.60)$$

where $V_0 > 0$, $L > 0$. We can solve $H_1\psi_0 = E_0\psi_0$, $E_0 \in \mathbb{R}$ separately for $x < -L$, for $|x| \leq L$ and for $x > L$. We obtain ψ_0 , which will play the role of a seed solution. We fix the following seed solution

$$\psi_0(x) = \begin{cases} A_1 e^{K_0 x}, & x < -L \\ B_1 \cos(k_0 x) + B_2 \sin(k_0 x), & |x| < L \\ C_1 e^{-K_0 x}, & x > L, \end{cases} \quad (2.61)$$

where we have defined $K_0 = \sqrt{V_0 - E_0}$, $k_0 = \sqrt{E_0}$. We can calculate W given by (2.12). The seed solution $f \equiv \psi_0$ is defined on intervals, the same is true for W . The formula for W is

$$W(x) = \begin{cases} -K_0, & x < -L \\ -k_0 \left(\frac{-B_1 \sin(k_0 x) + B_2 \cos(k_0 x)}{B_1 \cos(k_0 x) + B_2 \sin(k_0 x)} \right), & |x| < L \\ K_0, & x > L. \end{cases} \quad (2.62)$$

The new potential V_2 can be obtained from (2.20) where we set V_1 as (2.60). The potential V_2 is

$$V_2(x) = \begin{cases} V_0, & x < -L \\ 2k_0^2 \left[1 + \left(\frac{-B_1 \sin(k_0 x) + B_2 \cos(k_0 x)}{B_1 \cos(k_0 x) + B_2 \sin(k_0 x)} \right)^2 \right], & |x| < L \\ V_0, & x > L. \end{cases} \quad (2.63)$$

We focus on the calculation of square-integrable eigenstates of $H_2 = -\partial_x^2 + V_2$. We will obtain them by action of the operator \hat{A} (see (2.12)) on a solution of $H_1\psi = E\psi$. We fix ψ in this form

$$\psi(x) = \begin{cases} D e^{Kx}, & x < -L \\ A \cos(kx) + B \sin(kx), & |x| < L \\ F e^{-Kx}, & x > L. \end{cases} \quad (2.64)$$

Again, $K = \sqrt{V_0 - E}$, $k = \sqrt{E}$. The intertwining relation (2.17) and the resultant equation (2.19) give candidates on the eigenstates of H_2 . They are functions $\hat{A}\psi$. We act with the operator $\hat{A} = \partial_x + W$ on ψ ,

$$(\hat{A}\psi)(x) = \begin{cases} D(K - K_0)e^{Kx}, & x < -L \\ k[-A \sin(kx) + B \cos(kx)] + W[A \cos(kx) + B \sin(kx)], & |x| < L \\ -F(K - K_0)e^{-Kx}, & x > L. \end{cases} \quad (2.65)$$

We see that the function $\hat{A}\psi$ is square-integrable only when $K = \sqrt{V_0 - E} > 0$. That is the reason why we fixed ψ as the real exponential with the corresponding sign on each interval. We shall fix the coefficients such that the boundary conditions are satisfied. We require the continuity of $\hat{A}\psi$ and its derivation in $\pm L$,

$$\begin{aligned} \lim_{x \rightarrow \pm L^+} \hat{A}\psi(x) &= \lim_{x \rightarrow \pm L^-} \hat{A}\psi(x), \\ \lim_{x \rightarrow \pm L^+} (\hat{A}\psi)'(x) &= \lim_{x \rightarrow \pm L^-} (\hat{A}\psi)'(x). \end{aligned} \quad (2.66)$$

Substitution of (2.65) to (2.66) gives

$$\begin{aligned}
 (K_0 - K)e^{-KL}F &= \left. \frac{d\psi}{dx} \right|_{x=L} + W(L)\psi(L) \\
 -(K_0 - K)e^{-KL}D &= \left. \frac{d\psi}{dx} \right|_{x=-L} + W(-L)\psi(-L) \\
 -K(K_0 - K)e^{-KL}F &= -k^2\psi(L) + [W(x)\psi(x)]' \Big|_{x=L} \\
 -K(K_0 - K)e^{-KL}D &= -k^2\psi(-L) - [W(x)\psi(x)]' \Big|_{x=-L}.
 \end{aligned} \tag{2.67}$$

These are four equations for the unknown A, B, D, F , which determine the eigenstate (2.65). The determinant equal zero gives us the dispersion relation $E = E(k)$. Being the determinant of 4×4 matrix, it is hardly analytically solvable in general.

We shall discuss two special cases in which we can easily find solutions. In the first example, we set $B_1 = 0$. The formulas (2.65), (2.62) become much simpler. Later, we do the same with $B_2 = 0$. We will discuss these two special cases separately in the following two subsections.

2.5.1 Regularized $\sec^2(k_0x)$

With $B_2 = 0$ the potential V_2 and W , see (2.63) and (2.62), respectively, are

$$V_2(x) = \begin{cases} V_0, & x < -L \\ 2k_0^2 \frac{1}{\cos^2(k_0x)}, & |x| < L \\ V_0, & x > L \end{cases}, \quad W(x) = \begin{cases} -K_0, & x < -L \\ k_0 \operatorname{tg}(k_0x), & |x| < L \\ K_0, & x > L. \end{cases} \tag{2.68}$$

In general, the potential (2.68) can be singular. It will be regular only when $k_0x \in (-\frac{\pi}{2}, \frac{\pi}{2})$ for all $x \in [-L, L]$. It can happen when

$$k_0L \in (0, \frac{\pi}{2}). \tag{2.69}$$

In this case, the singularities of $\sec(k_0x)$ in the interval $[-L, L]$ are avoided. We choose only those $k_0 = E_0^2$, which fulfill (2.69).

The other problem is that the potential (2.68) is generally not continuous. For the continuity of (2.68) in the point $\pm L$, there must hold $\lim_{x \rightarrow \pm L^+} V_2(x) = \lim_{x \rightarrow \pm L^-} V_2(x)$ which is explicitly

$$\lim_{x \rightarrow \pm L^\mp} V_2(x) = \lim_{x \rightarrow \pm L^\mp} \frac{2k_0^2}{\cos^2(k_0x)} = V_0. \tag{2.70}$$

The adjustment process of k_0 to meet (2.70) is shown in Fig. 2.2. As we assumed that

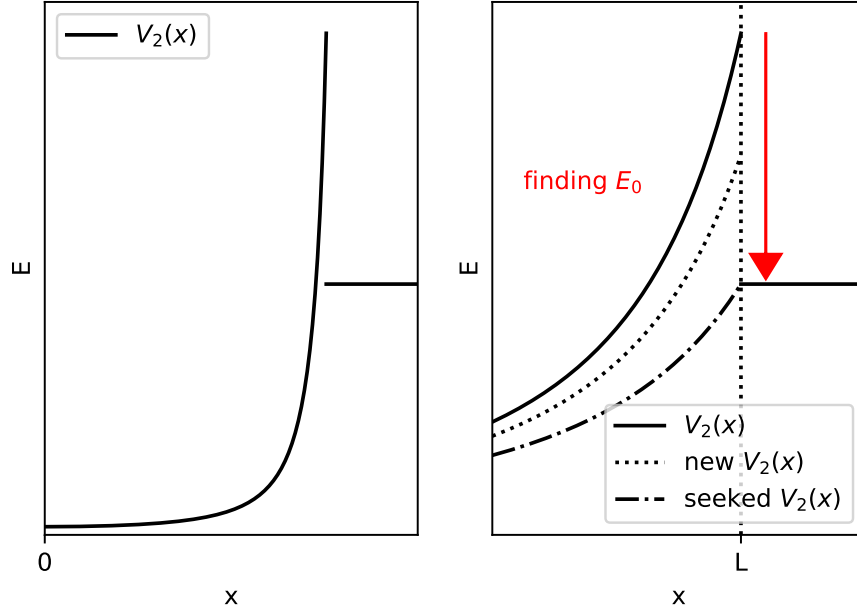


Figure 2.2: The potential (2.68) for $x > 0$ (left). In the detailed picture (right) is shown the process of regularization. We find $E_0 = k_0^2$ which makes the potential continuous.

(2.69) is valid, the potential V_2 has no singularities in $\pm L$. Therefore, we just put L into the limit, so

$$\frac{2k_0^2}{V_0} = \cos^2(k_0L). \quad (2.71)$$

From the equation, we will calculate $k_0 > 0$ numerically. It always has at least one solution k_0 , because we have k_0^2 and $\cos^2(k_0L)$ as functions of k_0 . One increases from $k_0 = 0$ to infinity, the latter decreases from 1 to 0.

We want to satisfy b.c. in (2.66). For that, we need the eigenfunctions $\hat{A}\psi$. The potential V_2 is even. We can find the solution as the even and odd parts of $\hat{A}\psi$. Here, $\hat{A}\psi$ is simply acquired from (2.65) where we set $B_2 = 0$

$$(\hat{A}\psi)(x) = \begin{cases} D(K - K_0)e^{Kx}, & x < -L \\ k[-A\sin(kx) + B\cos(kx)] + k_0\text{tg}(k_0x)(A\cos(kx) + B\sin(kx)), & |x| < L \\ -F(K - K_0)e^{-Kx}, & x > L. \end{cases} \quad (2.72)$$

Firstly, we extract the even part of $\hat{A}\psi$ as

$$(\hat{A}\psi)_{\text{even}}(x) = \begin{cases} D(K - K_0)e^{Kx}, & x < -L \\ kB\cos(kx) + k_0\text{tg}(k_0x)B\sin(kx), & |x| < L \\ D(K - K_0)e^{-Kx}, & x > L. \end{cases} \quad (2.73)$$

B.c. (2.66) are reduced to two equations for the point L , namely

$$\begin{aligned}\lim_{x \rightarrow L^+} \hat{A}\psi(x) &= \lim_{x \rightarrow L^-} \hat{A}\psi(x) \\ \lim_{x \rightarrow L^+} (\hat{A}\psi)'(x) &= \lim_{x \rightarrow L^-} (\hat{A}\psi)'(x).\end{aligned}\tag{2.74}$$

Substituting (2.73) to (2.74), we come to

$$\begin{aligned}D(K - K_0)e^{-KL} &= Bk\cos(kL) + Bk_0\text{tg}(k_0L)\sin(kL) \\ -DK(K - K_0)e^{-KL} &= -Bk^2\sin(kL) + \frac{Bk_0^2}{\cos^2(k_0L)}\sin(kL) + Bk_0k\text{tg}(k_0L)\cos(kL).\end{aligned}\tag{2.75}$$

There is $D(K - K_0)e^{-KL}$ in both equations. For this expression, we substitute the first equation to the second one and we get

$$\left[-k^2 + \frac{k_0^2}{\cos^2(k_0L)} + Kk_0\text{tg}(k_0L)\right]\sin(kL) = -[kK + k_0k\text{tg}(k_0L)]\cos(kL).\tag{2.76}$$

After that, we use (2.71) and two more identities

$$\cos(k_0L) = \frac{\sqrt{2}k_0}{\sqrt{V_0}}, \quad \text{tg}(k_0L) = \sqrt{\frac{1 - \cos^2(k_0L)}{\cos^2(k_0L)}}, \quad K^2 + k^2 = V_0.\tag{2.77}$$

Then, (2.76) simplifies to

$$\left[\frac{V_0}{2} - k^2 + K\sqrt{\frac{V_0}{2} - k_0^2}\right]\sin(kL) = -k\left[K + \sqrt{\frac{V_0}{2} - k_0^2}\right]\cos(kL).\tag{2.78}$$

This equation for $k^2 = E$ must be solved numerically. The relationship between constants D, B is obvious from the first equation of (2.75). Eventually, one optional constant is left. It is fully determined by the normalization of $(\hat{A}\psi)_{\text{even}}$.

We proceed in the same way for the odd part of $\hat{A}\psi$

$$(\hat{A}\psi)_{\text{odd}}(x) = \begin{cases} D(K - K_0)e^{Kx}, & x < -L \\ -kA\sin(kx) + k_0\text{tg}(k_0x)A\cos(kx), & |x| < L \\ -D(K - K_0)e^{-Kx}, & x > L. \end{cases}\tag{2.79}$$

The secular equation for the odd solution is

$$\left[\frac{V_0}{2} - k^2 + K\sqrt{\frac{V_0}{2} - k_0^2}\right]\cos(kL) = k\left[K + \sqrt{\frac{V_0}{2} - k_0^2}\right]\sin(kL).\tag{2.80}$$

Likewise in the even case, the equation does not support a solution for $E < 0$. The reason is simple. When $E < 0$ then $k = \sqrt{E} = i\sqrt{-E} = i\kappa$ is purely imaginary. Substituting $k = i\kappa, K = \sqrt{V_0 + \kappa^2}$ to (2.80), we obtain

$$\left[\frac{V_0}{2} + \kappa^2 + \sqrt{V_0 + \kappa^2}\sqrt{\frac{V_0}{2} - k_0^2}\right] = -\kappa\left[\sqrt{V_0 + \kappa^2} + \sqrt{\frac{V_0}{2} - k_0^2}\right]\text{tgh}(\kappa L).\tag{2.81}$$

Assuming $\kappa > 0$, the left-hand side is always positive and the right-hand side is always negative. Therefore, there does not exist a solution $\kappa > 0$. Both sides of the equation are even functions of κ . Thus, the solution $\kappa < 0$ is also not possible. Overall, $k = \sqrt{E} \in \mathbb{R}$ and must be found numerically.

From the form of eigenfunctions (2.73), (2.79) we see that E are limited above by V_0 . Otherwise, the eigenstates are not square-integrable ($K = \sqrt{V_0 - E}$). As was shown, the energies $E = k^2$ are limited from below by 0. It turns out that the system has a finite number of bound states. This is because oscillating and polynomial functions occur in the energy dispersion and the domain of energies is bounded, $E \in (0, V_0)$. The factorization energy E_0 must satisfy $\frac{2E_0}{V_0} < 1$, because (2.71) has a solution when $\frac{2E_0}{V_0} < 1$. Only then, the potential can be continuous. When $E_0 \rightarrow \frac{V_0}{2}$, we can find less energies (less bound states), because we push the lower limit closer to V_0 . When we did not insist on the continuous potential, the bound states could be found too. The benefit of continuous potential is also simplification of the dispersion relation, compare (2.76) with (2.78). The particular system is shown in Fig. 2.3.

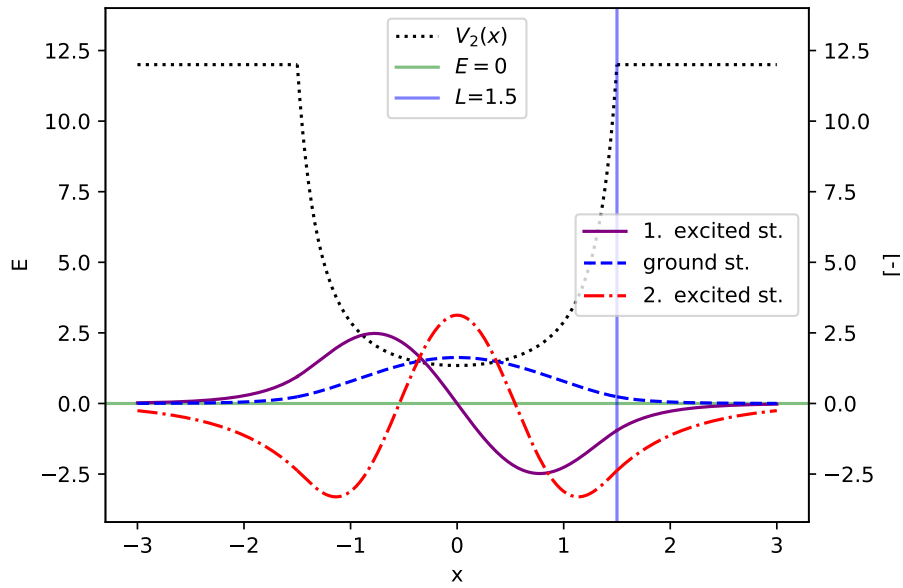


Figure 2.3: The regularized potential $V_2(x)$ (2.68) with the eigenfunctions (2.73), (2.79). The energy of the seed solution is $k_0^2 = E_0 = 0.6719$. The parameters of the well are $V_0 = 12$, $L = 1.5$. The energy for the ground state is $E_{gr} = 2.6525$, for the first excited state is $E_1 = 5.8103$ and for the second excited state is $E_2 = 9.7792$.

2.5.2 Regularized $\csc^2(kx)$

Now, let us discuss the second specific case where $B_1 = 0$ in (2.63). V_2 and W are given by

$$V_2(x) = \begin{cases} V_0, & x < -L \\ 2k_0^2 \frac{1}{\sin^2(k_0x)}, & |x| < L \\ V_0, & x > L \end{cases}, \quad W(x) = \begin{cases} -K_0, & x < -L \\ -k_0 \cotg(k_0x), & |x| < L \\ K_0, & x > L. \end{cases} \quad (2.82)$$

At first glance, the potential V_2 has the singular point in $x = 0$. It can have more singular points $\{x_i | i \in \hat{n}, n \in \mathbb{N}\}$ which are solutions of $\sin(k_0x_i) = 0$. We will require that V_2 has the only singular point $x = 0$. With respect to this requirement, we have to select the factorization energy E_0 such that

$$\sqrt{E_0}L \in (0, \pi) \implies \sin(k_0L) \neq 0. \quad (2.83)$$

In general, the potential V_2 is not continuous. We would like to fix k_0 such that V_2 is continuous in $x = \pm L$. Such k_0 has to satisfy

$$\frac{2k_0^2}{\sin^2(k_0L)} = V_0. \quad (2.84)$$

The process of making V_2 continuous will be the same as in 2.5.1. We just find the energy E_0 , which enables

$$\frac{2k_0^2}{V_0} = \sin^2(k_0L). \quad (2.85)$$

This is an equation for an unknown k_0 . It always has a solution. Maximal k_0 is limited by the condition $1 \geq \frac{2k_0^2}{V_0}$. Both functions k_0^2 , $\sin^2(k_0L)$ are zero for $k_0 = 0$. $\sin^2(k_0L)$ is a concave function and k_0^2 is a convex function. The function k_0^2 increases faster than $\sin^2(k_0L)$. Therefore, they have to intersect each other.

Again, (2.82) is an even function, so we will extract the even and odd parts of $\hat{A}\psi$. In addition, we shall not forget b.c. $(\hat{A}\psi)(0) = 0$ which follows from the singularity of V_2 in $x = 0$. Function $\hat{A}\psi$ is given by (2.65), where we set $B_1 = 0$

$$(\hat{A}\psi)(x) = \begin{cases} D(K - K_0)e^{Kx}, & x < -L \\ k[-A\sin(kx) + B\cos(kx)] - k_0 \cotg(k_0x) [A\cos(kx) + B\sin(kx)], & |x| < L \\ -F(K - K_0)e^{-Kx}, & x > L. \end{cases} \quad (2.86)$$

We start with the odd part of $\hat{A}\psi$

$$(\hat{A}\psi)_{\text{odd}}(x) = \begin{cases} D(K - K_0)e^{Kx}, & x < -L \\ -kA\sin(kx) - k_0A\cotg(k_0x) \cos(kx), & |x| < L \\ -D(K - K_0)e^{-Kx}, & x > L. \end{cases} \quad (2.87)$$

It is clear that it cannot be a solution. The problem is $\cotg(k_0x) \cos(kx)$, which always diverges in $x = 0$ ($k_0 \neq 0$) due to $\lim_{x \rightarrow 0} |\cotg(k_0x) \cos(kx)| = +\infty$. As was mentioned, it must hold $(\hat{A}\psi)_{\text{odd}}(0) = 0$. Let us move on to the even part of $\hat{A}\psi$

$$(\hat{A}\psi)_{\text{even}}(x) = \begin{cases} D(K - K_0)e^{Kx}, & x < -L \\ kB \cos(kx) - k_0 B \cotg(k_0x) \sin(kx), & |x| < L \\ D(K - K_0)e^{-Kx}, & x > L. \end{cases} \quad (2.88)$$

It satisfies $(\hat{A}\psi)_{\text{even}}(0) = 0$ and we substitute $(\hat{A}\psi)_{\text{even}}(x) = 0$ to (2.66)

$$\begin{aligned} D(K - K_0)e^{-KL} &= Ak \cos(kL) - Ak_0 \cotg(k_0L) \sin(kL) \\ -DK(K - K_0)e^{-KL} &= -Ak^2 \sin(kL) + \frac{Ak_0^2}{\sin^2(k_0L)} \sin(kL) - Ak_0 k \cotg(k_0L) \cos(kL). \end{aligned} \quad (2.89)$$

Substituting the first equation to the second one, we come to

$$\left[k^2 - \frac{k_0^2}{\sin^2(k_0L)} + Kk_0 \cotg(k_0L) \right] \text{tg}(kL) = [kK - kk_0 \cotg(k_0L)]. \quad (2.90)$$

It is an equation for possible energies $E = k^2$, which must be found numerically. Even without the explicit knowledge of E , $E < V_0$ must be valid to have (2.88) square-integrable. The particular system is shown in Fig. 2.4.

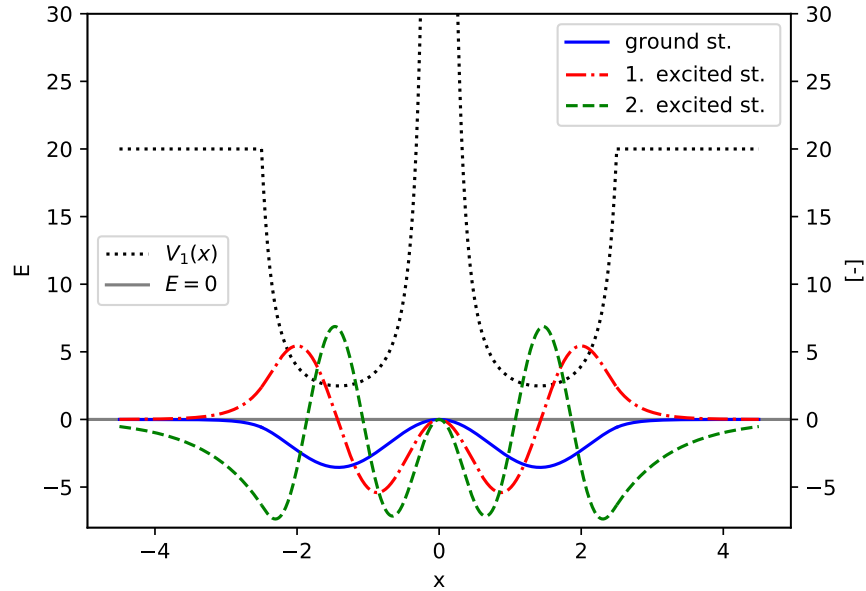


Figure 2.4: The regularized potential $V_2(x)$ of a type (2.82) with the eigenfunctions (2.88). The energy of the seed solution is $k_0^2 = E_0 = 1.23$ (given by (2.85)). The parameters of the well are $V_0 = 20$, $L = 2.5$. The energies are for the ground state $E_{gr} = 4.9144$, the first excited state $E_1 = 10.8703$ and the second excited state $E_2 = 18.4483$.

2.5.3 Spectra of FSW and its regularized versions

The spectra of systems with potentials (2.60), (2.68), (2.82) are in Fig. 2.5. The comparison of spectra revealed that FSW has more energy levels than both regularized wells. The lowest energy for FSW is missing in both \sec^2 , \csc^2 . In the spectrum of \sec^2 it corresponds to the factorization energy. The factorization energy of \csc^2 corresponds to the second energy level of FSW. Between two energy levels in the spectrum of \csc^2 , it always misses one energy level of FSW. This is because the wavefunctions of \csc^2 must satisfy b.c. in $x = 0$. The wavefunctions, which would theoretically have the missing energy similar to the FSW energy, do not fulfill it. Potentials \sec^2 , \csc^2 has energy levels slightly below those for FSW. Potential wells, which we approximate by FSW or \sec^2 , will have different ground states. In all mentioned potentials, the continuous spectrum is formed by energies $E \geq V_0$ (blue-filled rectangles). The thing, which is not evident from Fig. 2.5, is that the higher the energy E_0 (higher V_0 and well) is, the wider the energy gaps are.

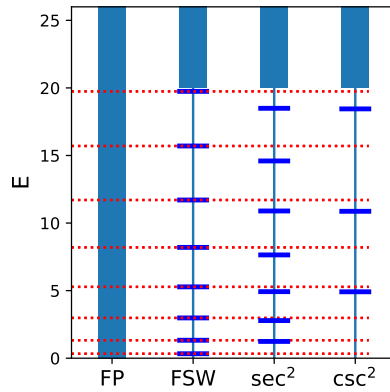


Figure 2.5: The comparison of spectra for the free particle $V(x) \equiv 0$ (FP), the finite square well (2.60) (FSW), the secant potential (2.68) (\sec^2) and the cosecant potential (2.82) (\csc^2). The parameters are $V_0 = 20$, $L = 2.5$ for all wells. The proper regularization of \sec^2 resp. \csc^2 wells is ensured by the factorization energy $E_0 = 0.31$ resp. $E_0 = 1.23$.

Chapter 3

DT for 1D Dirac operator

In this chapter, we will present the Darboux transformation for one-dimensional quantum systems described by the following dynamical equation

$$i\partial_t\psi = (-i\sigma_1\partial_x + V_1)\psi = H_1\psi, \quad (3.1)$$

where $V_1 = V_1(x)$ is a potential matrix, $\sigma_{1,2}$ are the Pauli matrices¹ and $\psi = (\psi_1, \psi_2)^T$ is a spinor. The time-independent 1D Dirac equation is

$$H_1\psi = (-i\sigma_1\partial_x + V_1)\psi = E\psi. \quad (3.3)$$

3.1 Matrix approach of DT

In this section, the results of [10] are summarized. We will work with $c = 1$, $\hbar = 1$. Let us assume that the Hamiltonians H_1, H_2 are intertwined by the operator \hat{A}

$$\hat{A}H_1 = H_2\hat{A} \quad (3.4)$$

and our purpose is to find \hat{A} and H_2 which satisfy the relation. We would like to have intertwined two 1D Dirac Hamiltonians, so

$$H_2 = -i\sigma_1\partial_x + V_2. \quad (3.5)$$

¹Pauli matrices

$$\sigma_1 = \begin{pmatrix} 0 & 1 \\ 1 & 0 \end{pmatrix}, \quad \sigma_2 = \begin{pmatrix} 0 & -i \\ i & 0 \end{pmatrix}, \quad \sigma_3 = \begin{pmatrix} 1 & 0 \\ 0 & -1 \end{pmatrix} \quad (3.2)$$

The Hamiltonian H_1 is the first-order operator, so its factorization is impossible. However, we can use the method to find \hat{A} analogous to 2.1. We make the following ansatz for the operator \hat{A} ,

$$\hat{A} = U\partial_x U^{-1} = \partial_x - U_x U^{-1}, \quad (3.6)$$

where $U_x = \partial_x U$. We substitute \hat{A} and H_2 into (3.4) and compare the matrix coefficients at the derivatives. There emerge two matrix equations for U and V_2 and we figure out how to find U and V_2 . We begin with U . The matrix U has to satisfy

$$H_1 U = U \lambda. \quad (3.7)$$

λ has the property $\lambda = \text{diag}(\lambda_1, \lambda_2)$, $\lambda_{1,2} \in \mathbb{R}$. We see that U is the eigenmatrix of H_1 . If we compose U of spinors u_1, u_2

$$U = (u_1, u_2), \quad (3.8)$$

they are acquired from

$$H_1 u_{1,2} = \lambda_{1,2} u_{1,2}. \quad (3.9)$$

Overall, spinors u_1, u_2 form the columns of U and they are the eigenstates of H_1 for the eigenvalues λ_1, λ_2 . It remains to determine V_2 . The newly created potential is

$$V_2 = V_1 - i \left[\sigma_1, U_x U^{-1} \right]. \quad (3.10)$$

The commutation relation of Pauli's matrices impose that newly created parts are only σ_2, σ_3 types and we cannot obtain σ_0, σ_1 . Compared to the DT for Schrödinger's operator, where we choose one factorization energy, the DT for the Dirac operator opens the way to various possibilities of V_2 thanks to two factorization energies $\lambda_{1,2}$.

Intertwining relations (3.4) help us to find a solution of $H_2 \varphi = E \varphi$ as follows

$$H_2 \hat{A} \psi = \hat{A} H_1 \psi = E \hat{A} \psi. \quad (3.11)$$

Here we use the fact that ψ is the eigenfunction of H_1 with the eigenvalue E . Specialty of the DT for the Dirac operator are missing states. They are energy levels λ_1, λ_2 which can or do not have to appear in the new transformed system. Path of their search begins with

$$\mathcal{V} = \left(U^\dagger \right)^{-1} = (v_1, v_2). \quad (3.12)$$

The matrix \mathcal{V} satisfy

$$H_2 \mathcal{V} = \mathcal{V} \lambda \iff H_2 v_{1,2} = \lambda_{1,2} v_{1,2}. \quad (3.13)$$

Spinors $v_{1,2}$ are the eigenstates of H_2 for the eigenvalues $\lambda_{1,2}$. Whether the energy levels $\lambda_{1,2}$ appear in the new system depends on what we require from $v_{1,2}$ (square-integrable, b.c. and so on). There always exist second linearly-independent solutions $\tilde{v}_{1,2}$ to $v_{1,2}$ which also satisfy $H_2 \tilde{v}_{1,2} = \lambda_{1,2} \tilde{v}_{1,2}$. For the Hamiltonian $H_2 = -i\sigma_1 \partial_x + A(x)\sigma_2 + M(x)\sigma_3$, the spinor $\tilde{v}_1 = (\tilde{v}_{11}, \tilde{v}_{12})^T$ is the second-linearly independent solution to $v_1 = (v_{11}, v_{12})^T$, $v_{11} \neq 0$ and can be calculated via

$$\begin{aligned} \tilde{v}_{11} &= -iv_{11} \int^x \frac{\lambda_1 + M(t)}{v_{11}^2(t)} dt \\ \tilde{v}_{12} &= -iv_{12} \int^x \frac{\lambda_1 + M(t)}{v_{11}^2(t)} dt - \frac{1}{v_{11}}. \end{aligned} \quad (3.14)$$

When $v_{11} \equiv 0$, we simultaneously interchange $v_{11} \leftrightarrow v_{12}$, $\tilde{v}_{11} \leftrightarrow \tilde{v}_{12}$ in the formulas.

The benefit of the Darboux transformation is that it produces the new solvable 1D Dirac systems. The eigenvalue equation of the new Dirac Hamiltonian $H_2\varphi = E\varphi$, as a differential equation, could be hardly solvable without the knowledge of intertwined Hamiltonians. Apparently, the Darboux transformation in 1D does not enable construction of $V = V(x, y)$, but it only enables $V = V(x)$. Higher-order Darboux transformations can be introduced. We apply the DT on a system number 1 and get a system number 2. Application of another DT on the system 2 gives us a system number 3. It can be repeated over and over again and reach the desired order of the transformation.

3.2 DT of free Dirac particle

Likewise with the Schrödinger operator, we can get off the mark from the DT of the free Dirac particle Hamiltonian to create non-trivial potentials. Let us solve the stationary eq. (3.3) for the free particle Hamiltonian $H_1 = -i\sigma_1\partial_x + m\sigma_2$. Here, $m \in \mathbb{R}$ is the mass of the particle. The eq. (3.3) can be rewritten into the following system of coupled equations for the spinor components

$$\begin{aligned} H_1\psi = (-i\sigma_1\partial_x + m\sigma_2)\psi = E\psi, \quad & -i\psi_2' - im\psi_2 = E\psi_1 \\ & -i\psi_1' + im\psi_1 = E\psi_2. \end{aligned} \quad (3.15)$$

We have to discuss two cases $E^2 = m^2$, $E^2 \neq m^2$. Starting with $E^2 \neq m^2$ the general solution is

$$\begin{pmatrix} \psi_1 \\ \psi_2 \end{pmatrix} = C_1 e^{ikx} \begin{pmatrix} m + ik \\ iE \end{pmatrix} + C_2 e^{-ikx} \begin{pmatrix} m - ik \\ iE \end{pmatrix}, \quad C_1, C_2 \in \mathbb{C}, \quad k = \sqrt{E^2 - m^2}. \quad (3.16)$$

Notice that k is real for $E^2 > m^2$ and purely imaginary for $E^2 < m^2$. In the second case $E^2 = m^2$, the solution is degenerated. For $E = m$ we have

$$\begin{pmatrix} \psi_1 \\ \psi_2 \end{pmatrix} = C_3 \begin{pmatrix} mx \\ imx - i \end{pmatrix} + C_4 \begin{pmatrix} 1 \\ i \end{pmatrix}, \quad C_3, C_4 \in \mathbb{C}. \quad (3.17)$$

The solution for $E = -m$ is

$$\begin{pmatrix} \psi_1 \\ \psi_2 \end{pmatrix} = C_5 \begin{pmatrix} mx \\ -imx + i \end{pmatrix} + C_6 \begin{pmatrix} 1 \\ -i \end{pmatrix}, \quad C_5, C_6 \in \mathbb{C}. \quad (3.18)$$

Due to the fact $\sigma_3 H_1 \sigma_3 = -H_1$, if we have a solution $H_1\psi = E\psi$, it is granted that $\sigma_3\psi$ solves $H_1\sigma_3\psi = -E\sigma_3\psi$. In [24], it states that it is *chiral symmetry*.

Let us discuss the DT of free particle systems. In the construction, fixing factorization energies plays a fundamental role. In dependence on their choice, we can expect exponentially decaying/increasing, sine/cosine or polynomial potentials. We define spinors

$$u_1(x) = \psi(x, E) \Big|_{E=\lambda_1}, \quad u_2(x) = \psi(x, E) \Big|_{E=\lambda_2}, \quad (3.19)$$

where $\psi(x, E)$ is the solution of differential equations (3.15), i.e. one of (3.16)-(3.18). We will present two explicit examples.

3.2.1 DT of free Dirac particle - example 1

We fix $\lambda_1 = m$, $\lambda_2 = \varepsilon \in (-m, m)$. Let us denote $P_\varepsilon = \varepsilon + m$, $K_\varepsilon = \sqrt{m^2 - \varepsilon^2}$. The appropriate selection of constants C_i enables us to write u_1, u_2 in the following form,

$$\begin{aligned} u_1(x) &= \psi(x, E) \Big|_{E=\lambda_1} = \frac{\mathbb{I} + i\sigma_1}{\sqrt{2}} \begin{pmatrix} 1 \\ 0 \end{pmatrix} = \begin{pmatrix} 1 \\ i \end{pmatrix}, \\ u_2(x) &= \psi(x, E) \Big|_{E=\lambda_2} = \frac{\mathbb{I} + i\sigma_1}{\sqrt{2}} \begin{pmatrix} -\frac{\text{sh}(K_\varepsilon x)}{K_\varepsilon} \\ \frac{i}{P_\varepsilon} \text{ch}(K_\varepsilon x) \end{pmatrix}. \end{aligned} \quad (3.20)$$

Finally, we create the matrix $U_x U^{-1}$ as defined in (3.8)

$$U_x U^{-1} = (u_1, u_2)_x (u_1, u_2)^{-1} = \frac{\mathbb{I} + i\sigma_1}{\sqrt{2}} \begin{pmatrix} 0 & iP_\varepsilon \\ 0 & K_\varepsilon \text{tgh}(K_\varepsilon x) \end{pmatrix} \frac{\mathbb{I} - i\sigma_1}{\sqrt{2}}. \quad (3.21)$$

The operator \hat{A} is with the use of (3.6)

$$\begin{aligned} \hat{A} &= \partial_x - \frac{\mathbb{I} + i\sigma_1}{\sqrt{2}} \begin{pmatrix} 0 & iP_\varepsilon \\ 0 & K_\varepsilon \text{tgh}(K_\varepsilon x) \end{pmatrix} \frac{\mathbb{I} - i\sigma_1}{\sqrt{2}} = \\ &= \partial_x - \begin{pmatrix} K_\varepsilon \text{tgh}(K_\varepsilon x) + P_\varepsilon & i(P_\varepsilon + K_\varepsilon \text{tgh}(K_\varepsilon x)) \\ i(P_\varepsilon - K_\varepsilon \text{tgh}(K_\varepsilon x)) & K_\varepsilon \text{tgh}(K_\varepsilon x) - P_\varepsilon \end{pmatrix}. \end{aligned} \quad (3.22)$$

The action of \hat{A} on an eigenfunction $\psi = (\psi_1, \psi_2)^T$ leads to

$$\phi = \hat{A}\psi = \begin{pmatrix} \psi'_1 - \frac{1}{2}(K_\varepsilon \text{tgh}(K_\varepsilon x) + P_\varepsilon)(\psi_1 + i\psi_2) \\ \psi'_2 + \frac{i}{2}(K_\varepsilon \text{tgh}(K_\varepsilon x) - P_\varepsilon)(\psi_1 + i\psi_2) \end{pmatrix}. \quad (3.23)$$

The Hamiltonian H_2 for the new system is (see (3.10))

$$H_2 = -i\sigma_1 \partial_x + V_2 = -i\sigma_1 \partial_x - \varepsilon \sigma_2 - \sqrt{m^2 - \varepsilon^2} \text{tgh}\left(x \sqrt{m^2 - \varepsilon^2}\right) \sigma_3. \quad (3.24)$$

The inhomogenous part of V_2 is represented by a parity odd function.

Notice that $\tilde{H}_1 = -i\sigma_1\partial_x + m\sigma_3$ can be transformed into $H_1 = -i\sigma_1\partial_x + m\sigma_2$ by the unitary transformation \mathbb{U} , that is, $\mathbb{U}\tilde{H}_1\mathbb{U}^\dagger = H_1$. It is represented in the matrix form as

$$\mathbb{U} = e^{i\frac{\pi}{4}\sigma_1} = \frac{1}{\sqrt{2}}(\mathbb{I} + i\sigma_1). \quad (3.25)$$

That is why most of the formulas above contain $\frac{1}{\sqrt{2}}(\mathbb{I} + i\sigma_1)$. For the need of other chapters, we also present (3.24), (3.23), (3.16) and (3.12) in their unitarily transformed form

$$\begin{aligned} \tilde{H}_2 &= \mathbb{U}^\dagger H_2 \mathbb{U} = -i\sigma_1\partial_x + \mathbb{U}V_2\mathbb{U}^\dagger = -i\sigma_1\partial_x - \varepsilon\sigma_3 + K_\varepsilon \operatorname{tgh}(K_\varepsilon x)\sigma_2, \\ \hat{A}\tilde{\psi} &= \begin{pmatrix} \psi'_1 - iP_\varepsilon\psi_2 \\ \psi'_2 - K_\varepsilon \operatorname{tgh}(K_\varepsilon x)\psi_2 \end{pmatrix}, \\ \tilde{\psi} &= C_1 e^{ikx} \begin{pmatrix} 1 \\ k \\ E+m \end{pmatrix} + C_2 e^{-ikx} \begin{pmatrix} 1 \\ k \\ -E+m \end{pmatrix} \\ \mathcal{V} &= (U^\dagger)^{-1} = \begin{pmatrix} \frac{P_\varepsilon}{K_\varepsilon} & 0 \\ i\frac{P_\varepsilon}{K_\varepsilon} \operatorname{tgh}(K_\varepsilon x) & \frac{iP_\varepsilon}{\operatorname{ch}(K_\varepsilon x)} \end{pmatrix}. \end{aligned} \quad (3.26)$$

3.2.2 DT of free Dirac particle - example 2

In the second presented example, we begin with a slightly changed free particle Hamiltonian $H_1 = -i\sigma_1\partial_x + m\sigma_3$. Its eigenfunctions $H_1\phi = E\phi$ are

$$\phi = C_1 e^{ikx} \begin{pmatrix} 1 \\ k \\ E+m \end{pmatrix} + C_2 e^{-ikx} \begin{pmatrix} 1 \\ k \\ -E+m \end{pmatrix}, \quad k^2 = E^2 - m^2, C_{1,2} \in \mathbb{C}. \quad (3.27)$$

In this section, we take $\lambda_1 = -\varepsilon \in (-m, 0)$, $\lambda_2 = \varepsilon \in (0, m)$, $m > 0$. The generating matrix U can be chosen as

$$U = \begin{pmatrix} \frac{i}{K_\varepsilon} \operatorname{sh}(K_\varepsilon x) & \frac{i}{K_\varepsilon} \operatorname{ch}(K_\varepsilon x) \\ \frac{1}{P_-} \operatorname{ch}(K_\varepsilon x) & \frac{1}{P_+} \operatorname{sh}(K_\varepsilon x) \end{pmatrix}. \quad (3.28)$$

The missing states v_1, v_2 are the columns of

$$\mathcal{V} = (v_1, v_2) = (U^\dagger)^{-1} = \frac{iK_\varepsilon^3}{m + \varepsilon \operatorname{ch}(2K_\varepsilon x)} \begin{pmatrix} -\frac{i}{P_+} \operatorname{sh}(K_\varepsilon x) & \frac{i}{P_-} \operatorname{ch}(K_\varepsilon x) \\ \frac{1}{K_\varepsilon} \operatorname{ch}(K_\varepsilon x) & \frac{1}{K_\varepsilon} \operatorname{sh}(K_\varepsilon x) \end{pmatrix}. \quad (3.29)$$

We have defined $P_\pm = m \pm \varepsilon$. The new Hamiltonian H_2 intertwined with H_1 is (see (3.10))

$$H_2 = -i\sigma_1\partial_x + V_2 = -i\sigma_1\partial_x + \left(m - \frac{K_\varepsilon^2}{m + \varepsilon \operatorname{ch}(2K_\varepsilon x)} \right) \sigma_3. \quad (3.30)$$

The potential is given in terms of an even function this time. The eigenfunctions ψ of the problem $H_2\psi = E\psi$ are

$$\begin{aligned} \psi &= (\partial_x - U_x U^{-1})\phi = \\ &= \begin{pmatrix} \phi_1' \\ \phi_2' \end{pmatrix} - \frac{1}{m + \varepsilon \operatorname{ch}(2K_\varepsilon x)} \begin{pmatrix} \varepsilon K_\varepsilon \operatorname{sh}(2K_\varepsilon x) & iK_\varepsilon^2 \\ -iK_\varepsilon^2 & \varepsilon K_\varepsilon \operatorname{sh}(2K_\varepsilon x) \end{pmatrix} \begin{pmatrix} \phi_1 \\ \phi_2 \end{pmatrix}. \end{aligned} \quad (3.31)$$

Chapter 4

Dirac equation in graphene

4.1 Description of crystals

Under the term crystal we can imagine a periodic arrangement of atoms. Crystals in nature are *real crystals*. On the other hand, we can work with a simplified crystal model, called the *ideal crystal*. Real crystals grow to a finite size. Their atom periodicity can be disturbed by crystal disorders, e.g. vacancy, where some atoms are missing in the expected positions. To make things easier, we will work with the ideal crystals. We take the ideal crystals as infinitely large objects. An ideal 3D crystal has translation symmetry along three independent directions $\vec{t}_1, \vec{t}_2, \vec{t}_3$. In two dimensions, we consider only two directions \vec{t}_1, \vec{t}_2 . We are heading to describe graphene, thus we will be interested mainly in 2D crystals.

4.2 Bravais lattice and crystal structure

We would like to give a detailed mathematical description of an infinitely large array of atoms. For that, we introduce the term of the *Bravais lattice*. It is defined as a set of points, whose position vector \vec{R} is

$$\vec{R} = n_1\vec{t}_1 + n_2\vec{t}_2 \equiv n_i\vec{t}_i, \quad \forall n_i \in \mathbb{Z}. \quad (4.1)$$

Vector \vec{R} does not have to correspond to the positions of the atoms. The part $\forall n_i \in \mathbb{Z}$ is also important, we cannot skip any index. In addition, it silently says that the set of points is infinitely large. The designation for \vec{t}_1, \vec{t}_2 is *primitive vectors*. The same Bravais lattice

can be generated by a different choice of primitive vectors. We find out that $\vec{t}_1 = 2\vec{t}_1 + \vec{t}_2$, $\vec{t}_2 = \vec{t}_2$ also create $\vec{R} = \tilde{n}_i \vec{t}_i$. We can produce different types of Bravais lattice just by changing the size of vectors and angles between them.

One of the types of Bravais lattice in 2D is the triangular Bravais lattice depicted in Fig. 4.1. The size of primitive vectors \vec{t}_1, \vec{t}_2 is the same, i.e. $|\vec{t}_1| = |\vec{t}_2|$. These two vectors are, in a certain sense, natural ones. They connect the nearest neighbors and minimize $|\vec{t}_1 \times \vec{t}_2|$ (area of the parallelogram). The vectors \vec{t}_1, \vec{t}_2 and \vec{t}_1, \vec{t}_2 generate the same Bravais lattice. It is similar to the case mentioned above, now the new vectors are $\vec{t}_1 = \vec{t}_1, \vec{t}_2 = 2\vec{t}_1 + \vec{t}_2$.

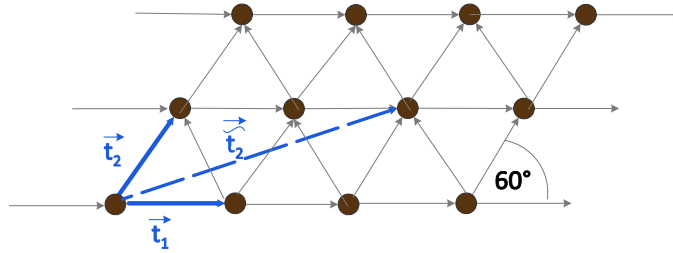


Figure 4.1: The triangular Bravais lattice.

The Bravais lattice reflects the periodicity of a crystal, not the position of atoms. *Basis* $\{\vec{d}_j \mid j = 1, 2, \dots, n \in \mathbb{N}\}$ is necessary to determine their positions. The Bravais lattice puts periodicity into play and vectors of the basis \vec{d}_j specify the position of atoms. The crystal structure is then a set of points

$$\vec{R}_j = n_i \vec{t}_i + \vec{d}_j, \quad \forall n_i \in \mathbb{Z}, j = 1, 2, \dots, n \in \mathbb{N}. \quad (4.2)$$

The points \vec{R}_j now coincide with the positions of the atoms. Graphene has a honeycomb lattice, see Fig. 4.2. The position of white circles (atoms *A*) is

$$\vec{R}_A = n_i \vec{t}_i + \vec{d}_1 = n_i \vec{t}_i + \vec{0} = n_i \vec{t}_i. \quad (4.3)$$

The position of black circles (atoms *B*) is

$$\vec{R}_B = n_i \vec{t}_i + \vec{d}_2 = \vec{R}_A + \vec{d}_2. \quad (4.4)$$

The explicit form of the primitive and basis vectors of the honeycomb lattice in Fig. 4.2 is

$$\vec{t}_1 = \frac{a}{2}(3, \sqrt{3}), \quad \vec{t}_2 = \frac{a}{2}(3, -\sqrt{3}), \quad \vec{d}_1 = \vec{0}, \quad \vec{d}_2 = (a, 0). \quad (4.5)$$

4.2.1 Wigner-Seitz cell

For other purposes, we present an idea of the *Wigner-Seitz cell*. Its construction is illustrated in Fig. 4.3. The general steps are following. We choose an arbitrary point of the

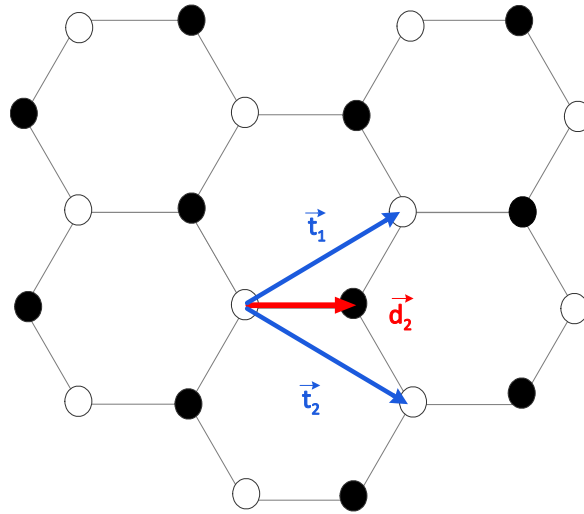


Figure 4.2: The honeycomb lattice.

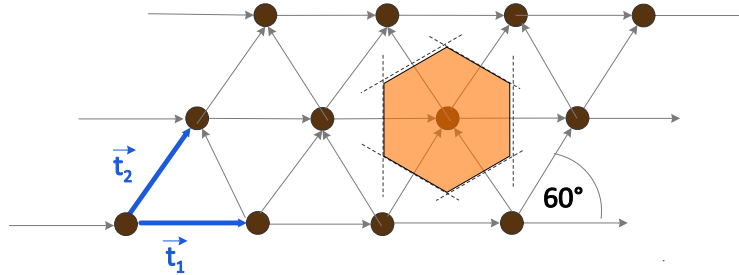


Figure 4.3: The Wigner-Seitz cell for the triangular lattice.

Bravais lattice. We take one of his nearest neighbors and draw a line halfway through them. It is perpendicular to their connecting line. We continue with the other nearest neighbors. The Wigner-Seitz cell is the smallest area delimited by the lines. Moving the Wigner-Seitz cell by $n_i \vec{t}_i$, we cover the whole space without overlap. Every point in the space can be described as

$$\vec{R} = \vec{w} + n_i \vec{t}_i. \quad (4.6)$$

The vector \vec{w} gives the position of a point in the Wigner-Seitz cell.

4.3 Reciprocal lattice

Primitive translation vectors of a reciprocal lattice $\vec{g}_1, \vec{g}_2, \vec{g}_3$ are defined by the condition

$$\vec{g}_i \cdot \vec{t}_j = 2\pi \delta_{ij}. \quad (4.7)$$

The Wigner-Seitz cell in the reciprocal space is called the *first Brillouine zone* (1BZ). Every vector \vec{g} of the reciprocal space can be decomposed to

$$\vec{g} = \vec{G} + \vec{k}, \quad \vec{k} \in 1\text{BZ}, \quad \vec{G} = m_i \vec{g}_i. \quad (4.8)$$

This relation points to the fact that 1BZ is exceptional. Knowledge of the 1BZ gives us the opportunity to express the whole reciprocal space. With use of (4.5) and (4.7), \vec{g}_1, \vec{g}_2 in the case of honeycomb lattice are

$$\vec{g}_1 = \frac{2\pi}{3a}(1, \sqrt{3}), \quad \vec{g}_2 = \frac{2\pi}{3a}(1, -\sqrt{3}). \quad (4.9)$$

4.4 Bloch's theorem

Finding a solution to the Schrödinger equation is not usually simple. Especially in a situation with complicated potential. The Bloch theorem says what form the wavefunctions have to have in a periodical potential

$$\psi(\vec{x} - \vec{a}) = e^{-i\vec{k} \cdot \vec{a}} \psi(\vec{x}). \quad (4.10)$$

We will prove this statement. Let us assume a periodical potential with a period \vec{a}

$$V(\vec{x}) = V(\vec{x} + \vec{a}). \quad (4.11)$$

The single particle Hamiltonian is

$$H = \frac{\vec{P}^2}{2M} + V(\vec{x}), \quad (4.12)$$

where \vec{P} is a momentum operator. In the following steps, we would like to apply the translation invariance of the crystal. More precisely, we will be interested in the translation invariance of the Bravais lattice. It seems useful to introduce a translational operator by relation

$$T_{\vec{a}} \psi(\vec{x}) = \psi(\vec{x} - \vec{a}). \quad (4.13)$$

It shifts the argument of the wave function by a constant vector \vec{a} . Operator $T_{\vec{a}}$ can be equivalently written as an exponential

$$T_{\vec{a}} = e^{-\frac{i}{\hbar} \vec{a} \cdot \vec{P}}. \quad (4.14)$$

Operators $H, T_{\vec{a}}$ commutes, we can find their common eigenfunctions ψ

$$\begin{aligned} H\psi &= E\psi \\ T_{\vec{a}}\psi &= \lambda_{\vec{a}}\psi. \end{aligned} \quad (4.15)$$

The normalization of $|\psi\rangle$ and the unitary operator $T_{\vec{a}}$ imply

$$1 = \langle T_{\vec{a}}\psi | T_{\vec{a}}\psi \rangle = |\lambda_{\vec{a}}|^2 \langle \psi | \psi \rangle = |\lambda_{\vec{a}}|^2. \quad (4.16)$$

The eigenvalue $\lambda_{\vec{a}}$ must lie on the unit circle

$$\lambda_{\vec{a}} = e^{if(\vec{a})}. \quad (4.17)$$

Here, $f(\vec{a})$ is an unknown function for now. Translation operators can be composed. It can be viewed (see (4.14) or (4.13)) that

$$T_{\vec{a}}T_{\vec{a}} = T_{2\vec{a}}, \quad T_{\vec{0}} = \hat{1}. \quad (4.18)$$

The application of the above mentioned expressions on eigenvectors ψ gives

$$f(2\vec{a}) = f(\vec{a}) + f(\vec{a}), \quad f(\vec{0}) = 0. \quad (4.19)$$

The function f is linear in \vec{a} . Because it appears in the exponent, it must be a scalar function. Simultaneously $f(\vec{0}) = 0$, so a good formula is

$$f(\vec{a}) = -\vec{k} \cdot \vec{a}, \quad \text{where } -\vec{k} = \overrightarrow{\text{const.}} \quad (4.20)$$

The relation $[H, T_{\vec{a}}] = 0$ and (4.15) say that when $H\psi = E\psi$ then $HT_{\vec{a}}\psi = ET_{\vec{a}}\psi$, where

$$\psi(\vec{x} - \vec{a}) = T_{\vec{a}}\psi(\vec{x}) = \lambda_{\vec{a}}\psi(\vec{x}) = e^{-i\vec{k} \cdot \vec{a}}\psi(\vec{x}). \quad (4.21)$$

The Bloch theorem claims that in a periodical potential the eigenfunctions must obey

$$\psi(\vec{x} - \vec{a}) = e^{-i\vec{k} \cdot \vec{a}}\psi(\vec{x}). \quad (4.22)$$

The Bloch theorem can be equivalently formulated in the speech of a periodic function $u_{\vec{k}}(\vec{x}) = u_{\vec{k}}(\vec{x} + \vec{a})$ [25],

$$\psi(\vec{x}) = e^{i\vec{k} \cdot \vec{x}}u_{\vec{k}}(\vec{x}). \quad (4.23)$$

This is the form of all wavefunctions in the periodic potential. The energy dispersion relation $E = E(\vec{k})$, also the *band structure*, arises from the Schrödinger equation. Crystals have the period $\vec{a} = n_i\vec{t}_i$. Thanks to the properties of reciprocal vectors (4.7), it holds true $(\vec{k} + m_j\vec{g}_j) \cdot n_i\vec{t}_i = \vec{k} \cdot n_i\vec{t}_i + m_jn_i2\pi\delta_{ij}$. Then, the exponential in (4.22) is $\exp(i(\vec{k} + m_j\vec{g}_j) \cdot n_i\vec{t}_i) = \exp(i\vec{k} \cdot n_i\vec{t}_i)$. We do not have to calculate $E(\vec{k})$ for all \vec{k} , but only for those \vec{k} from 1BZ.

4.5 Tight-binding model graphene

The exact solution of many-body problems is, with exceptions, impossible to find. That is why we have to accept approximate methods. Neglecting the electron-electron interaction

allows us to separate the total Hamiltonian H_{tot} to the sum of single electron Hamiltonians H , $H_{tot} = \sum H$. It suffices to focus on an electron in the potential of atom nuclei. In graphene, carbon has four valence electrons. Three participate in the C-C bond. The fourth is free and can move through the graphene layer. Thus, it is responsible for the electronic properties of graphene. The position of carbon atoms in the graphene layer was discussed in 4.2.

Imagine a single atom with only one free electron. The electron is described by a single particle Hamiltonian $H_0 = \frac{P^2}{2M} + V_0(\vec{x})$. Let us suppose that we can solve this problem. That means that we know $H_0\psi_{A,B} = E_{A,B}\psi_{A,B}$. Indices A, B distinguish atoms in different sublattices (different \vec{d}_A or \vec{d}_B), see 4.2. We would like to move on to the crystal, where more atoms are arranged. They are located at the positions $\vec{R}_{A,B} = \vec{d}_{A,B} + m_i\vec{t}_i$. All atoms in graphene are identical carbon atoms. Therefore, they generate a potential V_0 all alone. But the center of V_0 is shifted to $\vec{R}_{A,B}$, that is $V_0(\vec{x} - \vec{R}_{A,B})$. We know from the first paragraph that we may investigate only one electron. Its position is \vec{x} and its Hamiltonian

$$H = H_0 + \Delta V. \quad (4.24)$$

We denoted the potential contribution from other nuclei as ΔV . Our intention is to solve $H\Phi = E\Phi$ using $\psi_{A,B}$, $E_{A,B}$. We write the wavefunction of an electron Φ as a linear combination of all atomic orbitals ψ_A, ψ_B centred at the position of nuclei, namely

$$\begin{aligned} \Phi(\vec{x}) &= \frac{1}{\sqrt{2}}C_A \sum_{\vec{R}_A} a_{\vec{R}_A} \psi_A(\vec{x} - \vec{R}_A) + \frac{1}{\sqrt{2}}C_B \sum_{\vec{R}_B} b_{\vec{R}_B} \psi_B(\vec{x} - \vec{R}_B) = \\ &= C_A \frac{\mathcal{N}_1}{\sqrt{2}} \sum_{\vec{R}_A} e^{i\vec{k}\cdot\vec{R}_A} \psi_A(\vec{x} - \vec{R}_A) + C_B \frac{\mathcal{N}_1}{\sqrt{2}} \sum_{\vec{R}_B} e^{i\vec{k}\cdot\vec{R}_B} \psi_B(\vec{x} - \vec{R}_B) = \\ &= \frac{C_A\phi_A + C_B\phi_B}{\sqrt{2}}. \end{aligned} \quad (4.25)$$

The reason why we have written $a_{\vec{R}_A} = \mathcal{N}_1 e^{i\vec{k}\cdot\vec{R}_A}$, $b_{\vec{R}_B} = \mathcal{N}_1 e^{i\vec{k}\cdot\vec{R}_B}$, lies in the Bloch theorem 4.4. Due to the translation symmetry in the crystal, ϕ_A must satisfy the Bloch theorem. We can certainly rewrite the coefficient $a_{\vec{R}_A}$ as $\mathcal{N}_{\vec{R}_A} e^{i\vec{k}\cdot\vec{R}_A}$. The Bloch theorem implies

$$\begin{aligned} \phi_A(\vec{x} - m_i\vec{t}_i) &= \sum_{\vec{R}_A} \mathcal{N}_{\vec{R}_A} e^{i\vec{k}\cdot\vec{R}_A} \psi_A(\vec{x} - \vec{R}_A - m_i\vec{t}_i) = \\ &= \sum_{\vec{R}_A} \mathcal{N}_{\vec{R}_A} e^{i\vec{k}\cdot\vec{R}_A} \psi_A(\vec{x} - (\vec{R}_A + m_i\vec{t}_i)) e^{-im_i\vec{t}_i\cdot\vec{k}} e^{im_i\vec{t}_i\cdot\vec{k}} = \\ &= e^{-im_i\vec{t}_i\cdot\vec{k}} \sum_{\vec{r}_A} \mathcal{N}_{\vec{r}_A - m_i\vec{t}_i} \psi_A(\vec{x} - \vec{r}_A) \stackrel{!}{=} e^{-im_i\vec{t}_i\cdot\vec{k}} \phi_A(\vec{x}) = \\ &= e^{-im_i\vec{t}_i\cdot\vec{k}} \sum_{\vec{r}_A} \mathcal{N}_{\vec{r}_A} e^{i\vec{k}\cdot\vec{r}_A} \psi_A(\vec{x} - \vec{r}_A). \end{aligned} \quad (4.26)$$

Where we just renamed the summation parameter $\vec{r}_A = \vec{R}_A + n_i\vec{t}_i$, when passing from the second line to the third one. On the other hand, the last line must hold due to the Bloch theorem. Taking into account $\langle \psi_A(\vec{x} - m_i\vec{t}_i) | \psi_A(\vec{x} - n_i\vec{t}_i) \rangle \approx 0$, $n_i\vec{t}_i \neq m_i\vec{t}_i$, we obtain the

orthonormality of $\{\psi_A(\vec{x} - n_i \vec{t}_i)\}$. This approximation is feasible when ψ_A reaches zero quickly enough as the distance from $n_i \vec{t}_i$ increases. Comparing the coefficients term by term we get $\mathcal{N}_1 \equiv \mathcal{N}_{\vec{r}_A} = \mathcal{N}_{\vec{r}_A - n_i \vec{t}_i}, \forall n_{1,2,3} \in \mathbb{Z}$. All the constants $\mathcal{N}_{\vec{r}_A}$ are the same and we denote them \mathcal{N}_1 . Then ϕ_A is simplified to

$$\phi_A(x) = \mathcal{N}_1 \sum_{\vec{R}_A} e^{i\vec{k} \cdot \vec{R}_A} \psi_A(\vec{x} - \vec{R}_A). \quad (4.27)$$

The constant \mathcal{N}_1 also plays another role, it is a normalization constant. We proceed likewise for ϕ_B . Keep in mind that $\vec{R}_B = \vec{R}_A + \vec{d}_2$, see 4.2. Thus, the normalization constant for the B part is again \mathcal{N}_1 .

The energy of the electron in the state Φ is

$$\frac{\langle \Phi | H | \Phi \rangle}{\langle \Phi | \Phi \rangle} = E. \quad (4.28)$$

We have to determine E and C_A, C_B defined in (4.25). This can be done by finding the minimum of $E(\overline{C}_A, \overline{C}_B)$. Substituting (4.25) to (4.28) and differentiation with respect to $\overline{C}_A, \overline{C}_B$, we get

$$\begin{aligned} \sum_{j=A,B} \langle \phi_l | H | \phi_j \rangle C_j &= E \sum_{j=A,B} \langle \phi_l | \phi_j \rangle C_j, \quad \forall l \in \{A, B\} \\ \sum_{j=A,B} \mathbb{H}_{lj} C_j &= E \sum_{j=A,B} \mathbb{S}_{lj} C_j, \end{aligned} \quad (4.29)$$

where we have defined matrix elements $\mathbb{H}_{lj} = \langle \phi_l | H | \phi_j \rangle, \mathbb{S}_{lj} = \langle \phi_l | \phi_j \rangle$. The equation can be rewritten to a matrix form $(\mathbb{H} - ES)\vec{C} = 0$. The non-trivial solution can be found only when

$$\det(\mathbb{H} - ES) = 0. \quad (4.30)$$

We obtain energy E from this condition and then calculate C_j . It looks very simple, unfortunately, every rose has its thorn. The hard thing is to determine matrix elements of \mathbb{H} , resp. \mathbb{S} . Once again, we shall accept some approximations. Let us look at the matrix element

$$\langle \phi_A | H | \phi_A \rangle = \mathcal{N}_1^2 \sum_{\vec{R}'_A} \sum_{\vec{R}_A} e^{-i\vec{k} \cdot \vec{R}_A} e^{i\vec{k} \cdot \vec{R}'_A} \left\langle \psi_A(\vec{x} - \vec{R}_A) \left| H_0 + \Delta V \right| \psi_A(\vec{x} - \vec{R}'_A) \right\rangle. \quad (4.31)$$

We know that ψ_A are the eigenfunctions of H_0 with the eigenvalue E_A , i.e. $H_0 \psi_A = E_A \psi_A$. In addition, we make the following assumptions/approximations:

1. $\langle \psi_A(\vec{x} - \vec{R}_A) | \psi_A(\vec{x} - \vec{R}'_A) \rangle = \delta_{\vec{R}_A, \vec{R}'_A},$
2. $\langle \psi_B(\vec{x} - \vec{R}_B) | \psi_B(\vec{x} - \vec{R}'_B) \rangle = \delta_{\vec{R}_B, \vec{R}'_B},$
3. $\langle \psi_B(\vec{x} - \vec{R}_B) | \psi_A(\vec{x} - \vec{R}'_A) \rangle = 0,$

4. $\langle \psi_A(\vec{x} - \vec{R}_A) | \Delta V | \psi_A(\vec{x} - \vec{R}'_A) \rangle \approx 0$ (will be commented later),
5. $1 = |\phi_A|^2 = \mathcal{N}_1^2 \sum_{\vec{R}'_A} \sum_{\vec{R}_A} e^{-i\vec{k} \cdot \vec{R}_A} e^{i\vec{k} \cdot \vec{R}'_A} \langle \psi_A(\vec{x} - \vec{R}_A) | \psi_A(\vec{x} - \vec{R}'_A) \rangle$

We can set $\langle \psi_A(\vec{x} - \vec{R}_A) | \Delta V | \psi_A(\vec{x} - \vec{R}'_A) \rangle \approx 0$, because we expect the potential $V_0(\vec{x} - \vec{R}_A)$ and the wavefunction $\psi_A(\vec{x} - \vec{R}_A)$ localized at the position \vec{R}_A . The overlap of $\psi_A(\vec{x} - \vec{R}'_A)$ with $\psi_A(\vec{x} - \vec{R}_A)$ is for $\vec{R}'_A \neq \vec{R}_A$ approximately zero. When $\vec{R}'_A = \vec{R}_A$, then nuclei localized at some other positions than \vec{R}_A have not significant influence in \vec{R}_A , so $\Delta V \approx 0$ and $\langle \psi_A(\vec{x} - \vec{R}_A) | \Delta V | \psi_A(\vec{x} - \vec{R}'_A) \rangle \approx 0$. Then the matrix element $\mathbb{H}_{AA} = \langle \phi_A | H | \phi_A \rangle$ has a fine form

$$\mathbb{H}_{AA} = E_A. \quad (4.32)$$

The matrix element \mathbb{H}_{BB} is obtained by exchanging A with B

$$\mathbb{H}_{BB} = E_B = E_A. \quad (4.33)$$

The energies E_A, E_B cannot be diverse, because both sublattices A, B are made of the same carbon atoms, thus $E_A = E_B$.

Because of $\mathbb{H}_{BA} = \overline{\mathbb{H}_{AB}}$, it remains to calculate the off-diagonal element \mathbb{H}_{AB} which is

$$\langle \phi_A | H | \phi_B \rangle = \mathcal{N}_1^2 \sum_{\vec{R}_A} \sum_{\vec{R}_B} e^{-i\vec{k} \cdot \vec{R}_A} e^{i\vec{k} \cdot \vec{R}_B} \langle \psi_A(\vec{x} - \vec{R}_A) | H_0 + \Delta V | \psi_B(\vec{x} - \vec{R}_B) \rangle. \quad (4.34)$$

ψ_B are eigenfunctions of H_0 with the energy $E_B = E_A$. For graphene, it holds $\vec{R}_B = \vec{R}'_A + \vec{d}_2$. We denoted the second summation index as \vec{R}'_A , otherwise there would be a mess in the sums. The element \mathbb{H}_{AB} becomes

$$\begin{aligned} \mathbb{H}_{AB} &= \mathcal{N}_1^2 \sum_{\vec{R}_A} \sum_{\vec{R}'_A} e^{-i\vec{k} \cdot \vec{R}_A} e^{i\vec{k} \cdot (\vec{R}'_A + \vec{d}_2)} \langle \psi_A(\vec{x} - \vec{R}_A) | H | \psi_B(\vec{x} - \vec{R}'_A - \vec{d}_2) \rangle = \\ &= \mathcal{N}_1^2 \sum_{\vec{R}_A} \sum_{\vec{R}'_A} e^{-i\vec{k} \cdot \vec{R}_A} e^{i\vec{k} \cdot (\vec{R}'_A + \vec{d}_2)} \langle \psi_A(\vec{x} - \vec{R}_A) | E_A + \Delta V | \psi_B(\vec{x} - \vec{R}'_A - \vec{d}_2) \rangle = \\ &= \mathcal{N}_1^2 \sum_{\vec{R}_A} \sum_{\vec{R}'_A} e^{-i\vec{k} \cdot \vec{R}_A} e^{i\vec{k} \cdot (\vec{R}'_A + \vec{d}_2)} \langle \psi_A(\vec{x} - \vec{R}_A) | \Delta V | \psi_B(\vec{x} - \vec{R}'_A - \vec{d}_2) \rangle. \end{aligned} \quad (4.35)$$

The problematic part is with ΔV . We cannot neglect it, because the atoms A and B are closer to each other than the atoms A and A . Also, if we ignored it, we would get rid of any interaction in the system and $\mathbb{H} = E_A \mathbb{I}$. We choose one atom in the lattice. The most significant interaction is with the nearest atoms. In the *nearest neighbor approximation* (NN approximation), we assume that only the interaction with the nearest neighbors is non-vanishing. When we look at Fig. 4.2, we see that every black point has three white NNs and reversely. By fixing \vec{R}_A , then $\vec{R}'_A = \vec{R}_A$, $\vec{R}'_A = \vec{R}_A - \vec{t}_1$, $\vec{R}'_A = \vec{R}_A - \vec{t}_2$ are relevant in the sum (4.35). For the NNs, we define

$$t = \langle \psi_A(\vec{x} - \vec{R}_A) | \Delta V | \psi_B(\vec{x} - \vec{R}'_A - \vec{d}_2) \rangle \in \mathbb{R}, \quad (4.36)$$

so called *hopping parameter* t . Therefore, we get

$$\mathbb{H}_{AB} = \mathcal{N}_1^2 \sum_{\vec{R}_A} \sum_{\vec{R}'_A = \text{NN}} e^{-i\vec{k}\cdot\vec{R}_A} e^{i\vec{k}\cdot(\vec{R}'_A + \vec{d}_2)} t = e^{i\vec{k}\cdot\vec{d}_2} (1 + e^{-i\vec{k}\cdot\vec{t}_1} + e^{-i\vec{k}\cdot\vec{t}_2}) t. \quad (4.37)$$

Equipped with the matrix elements (4.32), (4.33) and (4.37), we can write \mathbb{H} in the following form

$$\mathbb{H} = \begin{pmatrix} E_A & te^{i\vec{k}\cdot\vec{d}_2} (1 + e^{-i\vec{k}\cdot\vec{t}_1} + e^{-i\vec{k}\cdot\vec{t}_2}) \\ te^{-i\vec{k}\cdot\vec{d}_2} (1 + e^{i\vec{k}\cdot\vec{t}_1} + e^{i\vec{k}\cdot\vec{t}_2}) & E_A \end{pmatrix}. \quad (4.38)$$

In (4.30), the *overlapping matrix* \mathbb{S} is unknown yet

$$\mathbb{S} = \begin{pmatrix} \langle \phi_A | \phi_A \rangle & \langle \phi_A | \phi_B \rangle \\ \langle \phi_B | \phi_A \rangle & \langle \phi_B | \phi_B \rangle \end{pmatrix}. \quad (4.39)$$

Analogously as for the matrix \mathbb{H} , we rewrite \vec{R}'_A as $\vec{R}'_A = \vec{R}_A$, $\vec{R}'_A = \vec{R}_A - \vec{t}_1$, $\vec{R}'_A = \vec{R}_A - \vec{t}_2$. We impose 4.5,

$$0 = \langle \psi_A(\vec{x} - \vec{R}_A) | \psi_B(\vec{x} - \vec{R}'_A - \vec{d}_2) \rangle. \quad (4.40)$$

The overlapping matrix is

$$\mathbb{S} = \begin{pmatrix} 1 & 0 \\ 0 & 1 \end{pmatrix}. \quad (4.41)$$

After exhausting evaluation of two matrices, we can finally solve (4.30)

$$0 = \det \begin{pmatrix} E_A - E & te^{i\vec{k}\cdot\vec{d}_2} [1 + e^{-i\vec{k}\cdot\vec{t}_1} + e^{-i\vec{k}\cdot\vec{t}_2}] \\ te^{-i\vec{k}\cdot\vec{d}_2} [1 + e^{i\vec{k}\cdot\vec{t}_1} + e^{i\vec{k}\cdot\vec{t}_2}] & E_A - E \end{pmatrix}. \quad (4.42)$$

We remark that $\vec{t}_1 = \frac{a}{2}(3, \sqrt{3})$ and $\vec{t}_2 = \frac{a}{2}(3, -\sqrt{3})$. The constant a is the distance between carbon atoms. We apply it to the determinant condition and we get

$$(E_A - E)^2 = t^2 \underbrace{\left[3 + 4\cos\left(\frac{3}{2}k_x a\right) \cos\left(\frac{\sqrt{3}}{2}k_y a\right) + 2\cos\left(\sqrt{3}k_y a\right) \right]}_{f(\vec{k})}. \quad (4.43)$$

As can be seen from Fig. 4.4, the function $f(\vec{k})$ vanishes in six points $\vec{k}_1, \dots, \vec{k}_6$. When we construct the 1BZ for the honeycomb lattice oriented as in Fig. 4.2, the vectors $\vec{k}_1, \dots, \vec{k}_6$ coincide with six corners of the 1BZ. They are called the *Dirac points*. Their property is $f(\vec{k}_i) = 0$, $i \in \hat{6}$, which means $E = E_A$ for (4.43). The function $f(\vec{k})$ is maximized (all cosines equal 1), when $\vec{k} = \vec{0}$. Only the two out of six Dirac points in the 1BZ are inequivalent. We denote them K, K' or \vec{K}, \vec{K}' . The remaining four points are equal to K, K' up to a shift with reciprocal lattice vectors.

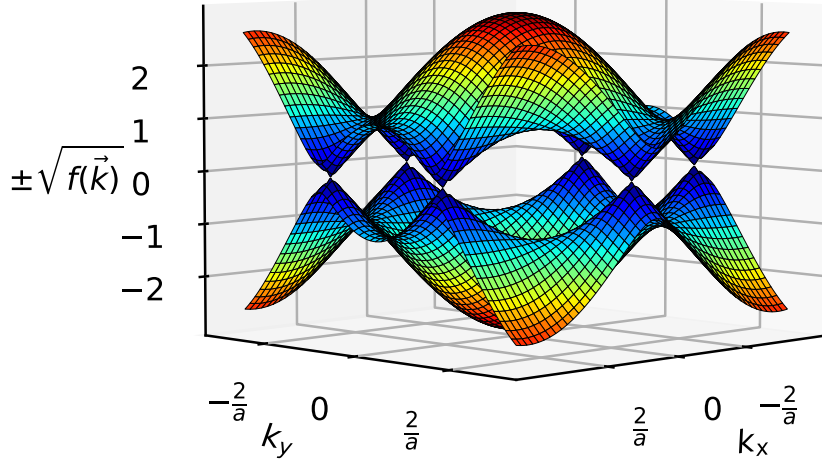


Figure 4.4: The functions $\pm\sqrt{f(\vec{k})}$ defined in (4.43), which are significant for the energy dispersion $E(\vec{k})$.

Electrons with the energy $E = E_A$ have \vec{k} near the Dirac point \vec{K} . Let us take $\vec{k} = \vec{K} + \vec{q}$, where $|\vec{q}| \ll |\vec{K}|$, and substitute it to (4.38)

$$\mathbb{H} = \begin{pmatrix} E_A & te^{i(\vec{K}+\vec{q})\cdot\vec{d}_2}(1 + e^{-i(\vec{K}+\vec{q})\cdot\vec{t}_1} + e^{-i(\vec{K}+\vec{q})\cdot\vec{t}_2}) \\ te^{-i(\vec{K}+\vec{q})\cdot\vec{d}_2}(1 + e^{i(\vec{K}+\vec{q})\cdot\vec{t}_1} + e^{i(\vec{K}+\vec{q})\cdot\vec{t}_2}) & E_A \end{pmatrix}. \quad (4.44)$$

We Taylor-expand the elements of Hamiltonian matrix. It will be performed in the vicinity of $\vec{K} = \frac{2\pi}{3\sqrt{3}a}(\sqrt{3}, 1)$ in the variable \vec{q} . We keep only the first order in \vec{q} , then

$$\begin{aligned} \mathbb{H} &\approx \begin{pmatrix} E_A & -\frac{3at}{2}e^{i\frac{5\pi}{6}}(q_x - iq_y) \\ -\frac{3at}{2}e^{-i\frac{5\pi}{6}}(q_x + iq_y) & E_A \end{pmatrix} = \\ &= E_A\mathbb{I} - \frac{3at}{2} \begin{pmatrix} 0 & e^{i\frac{5\pi}{6}}(q_x - iq_y) \\ e^{-i\frac{5\pi}{6}}(q_x + iq_y) & 0 \end{pmatrix}. \end{aligned} \quad (4.45)$$

The $q_{x,y}$ is related to the momentum $p_{x,y}$ as $\hbar q_{x,y} = p_{x,y}$. We work with $\hbar = 1$, so $q_{x,y} = p_{x,y}$. The principle of correspondence postulates $p_x \rightarrow -i\partial_x$, $p_y \rightarrow -i\partial_y$, so

$$\mathbb{H} \approx E_A\mathbb{I} - \frac{3at}{2} \begin{pmatrix} 0 & e^{i\frac{5\pi}{6}}(-i\partial_x - \partial_y) \\ e^{-i\frac{5\pi}{6}}(-i\partial_x + \partial_y) & 0 \end{pmatrix}. \quad (4.46)$$

For simplicity, we fix $v_f = \frac{3at}{2} = 1$. Index f denotes Fermi velocity - group velocity at $\vec{k} = \vec{K}$. We almost see the Dirac Hamiltonian in 2D $H_K = -i(\sigma_1\partial_x + \sigma_2\partial_y)$. The constant term $E_A\mathbb{I}$ only shifts the spectrum and will not affect the physics of electrons. The phase factor $e^{i\frac{5\pi}{6}}$ can be removed by the unitary transformation $\mathbb{U} = e^{-i\frac{5\pi}{12}\sigma_3}$.

After the corrections, the Hamiltonian for K in the TB approximation reads as

$$H_K = -i(\sigma_1 \partial_x + \sigma_2 \partial_y). \quad (4.47)$$

If we started with $\vec{K}' = \frac{2\pi}{3\sqrt{3}a}(\sqrt{3}, -1)$, the Hamiltonian would become

$$H_{K'} = -i(\sigma_1 \partial_x - \sigma_2 \partial_y). \quad (4.48)$$

The Hamiltonian, which takes into account both Dirac points is

$$\mathbb{H} = \begin{pmatrix} H_K & 0 \\ 0 & H_{K'} \end{pmatrix}. \quad (4.49)$$

The eigenfunctions of \mathbb{H} are $(\Psi_{AK}, \Psi_{BK}, \Psi_{AK'}, \Psi_{BK'})^T$. Sometimes it is more convenient to consider different order of components as $(\Psi_{AK}, \Psi_{BK}, \Psi_{BK'}, \Psi_{AK'})^T$ and the Hamiltonian

$$H = \begin{pmatrix} H_K & 0 \\ 0 & H_K \end{pmatrix} = \begin{pmatrix} H_K & 0 \\ 0 & \sigma_1 H_{K'} \sigma_1 \end{pmatrix} = -i\sigma_0 \otimes \sigma_1 \partial_x - i\sigma_0 \otimes \sigma_2 \partial_y. \quad (4.50)$$

We will work with H and the order of components belonging to it.

4.6 Interaction in graphene

Until here, we considered only free electrons. We introduce interaction potentials. We assume the potentials of one variable x . Later, it would be much more complicated to solve the potentials of two variables x, y . The interaction will be mediated by 2×2 matrices $V_K(x), V_{K'}(x)$. Universally, they can be different for different Dirac points. We assume only potentials preserving the block-diagonal form of Hamiltonians. Then, we generalize the free particle Hamiltonian (4.50), so we construct

$$H = \begin{pmatrix} H_K + V_K & 0 \\ 0 & H_K + V_{K'} \end{pmatrix}. \quad (4.51)$$

The Hamiltonian $\text{diag}(H_K, H_K)$ commutes with the time-reversal operator $\hat{\mathcal{T}}$ [15],

$$\hat{\mathcal{T}} = -\sigma_2 \otimes \sigma_2 \hat{C}, \quad \hat{\mathcal{T}}^2 = \mathbb{I}, \quad (4.52)$$

where \hat{C} represents conjugation. We start with the potentials $V(x)\sigma_2 = V_K(x) = V_{K'}(x)$ or $V(x)\sigma_2 = V_K(x) = -V_{K'}(x)$ where $V(x)$ is real-valued. In a compact form as 4×4 matrices, they are

$$A_y(x) = V(x)\sigma_0 \otimes \sigma_2, \quad \tilde{A}_y(x) = V(x)\sigma_3 \otimes \sigma_2. \quad (4.53)$$

It holds true $\hat{\mathcal{T}}A_y(x)\hat{\mathcal{T}}^\dagger = -A_y(x)$, where $\hat{\mathcal{T}}$ is the time-reversal operator defined in (4.52). Thus, it truly represents the vector potential $A_y(x)$, which determines the magnetic field

$B_z(x) = \partial_x A_y(x)$. The matrix $\tilde{A}_y(x)$ does not change the sign, i.e. $\hat{T}\tilde{A}_y(x)\hat{T}^\dagger = \tilde{A}_y(x)$ and it represents a pseudo-vector (pseudo-magnetic) field. Let us define two more potentials

$$M(x) = V(x)\sigma_3 \otimes \sigma_3, \quad \tilde{M}(x) = V(x)\sigma_0 \otimes \sigma_3. \quad (4.54)$$

Only $M(x)$ commutes with the time-reversal operator defined in (4.52). We consider it as a physically realizable mass. On the other hand, $\tilde{M}(x)$ has no physical meaning.

4.6.1 Pseudo-magnetic field

When we mechanically stretch a piece of graphene, we can change its electronic properties. Devices created by strain engineering are based on this idea. For example, we could open the gap or induce an effective pseudo-magnetic field inside the sample. Material deformations are described by 3×3 symmetrical matrix $u_{ij} = u_{ji}$ so called *deformation tensor* [14],

$$u_{ij} = \frac{1}{2} [\partial_i u_j + \partial_j u_i + (\partial_i h)(\partial_j h)]. \quad (4.55)$$

There occur horizontal displacement $\vec{u} = (u_1(x, y), u_2(x, y))$ and vertical displacement $h(x, y)$. For the perfect 2D plane geometry of graphene, $h(x, y) = 0$. Small deformations in horizontal directions arise when little stress is applied to the material. *Stress tensor* σ_{ij} is related to u_{ij} for small deformations,

$$\sigma_{ij} = \lambda \text{Tr}(u)\delta_{ij} + 2\mu u_{ij}. \quad (4.56)$$

Lamé coefficients λ, μ are material constants. The diagonal elements of σ_{ij} are *normal stress* and the off-diagonal represents *shear stress*. The strain field u_{ij} creates a pseudo-vector potential $\vec{A}(x, y) = (\tilde{A}_x(x, y), \tilde{A}_y(x, y))$ and a scalar potential $V(x, y)$ [5], [13],

$$\tilde{A}_x = \frac{\beta}{a}(u_{11} - u_{22}), \quad \tilde{A}_y = \frac{-2\beta}{a}u_{12}, \quad V = (u_{11} + u_{22})g. \quad (4.57)$$

The distance between relaxed atoms in the lattice is $a \approx 0.142$ nm. Factors β, g range between $\beta \approx 2 - 3$, $g \approx 0 - 20$ eV [14]. The Hamiltonian for valley K is

$$H_K = -i(\sigma_1\partial_x + \sigma_2\partial_y) + \tilde{A}_x\sigma_1 + \tilde{A}_y\sigma_2 + V\sigma_0. \quad (4.58)$$

Taking into account that deformations commute with the time-reversal operator, we can write the Hamiltonian for both Dirac points as follows

$$H = -i\sigma_0 \otimes (\sigma_1\partial_x + \sigma_2\partial_y) + \sigma_3 \otimes (\tilde{A}_x\sigma_1 + \tilde{A}_y\sigma_2) + V\sigma_0 \otimes \sigma_0. \quad (4.59)$$

4.6.2 Staggered potential

Let us clarify the meaning of a mass term

$$M(x) = V(x)\sigma_3 \otimes \sigma_3. \quad (4.60)$$

Considering bispinors $\Psi = (\Psi_{AK}, \Psi_{BK}, \Psi_{BK'}, \Psi_{AK'})^T$, the potential $V(x)$ interacts oppositely in sublattices A and B . Until now, we have pursued only graphene. It consists only of carbon atoms. Therefore, it is unusual for $M(x)$ to act differently in sublattices A, B . However, there exist materials which have a honeycomb lattice and each sublattice is composed of chemically diverse atoms. In addition, their charge carriers obey the Dirac equation, for example boron nitride from the group *two-dimensional transition metal dichalcogenides* [26]. Combining an external field and chemically dissimilar atoms results in a diverse potential in the sublattices - *staggered potential*. Its presence gives rise to the opening of a band gap. Manipulation of the band gap is essential for electronics.

Chapter 5

Nanoribbons

A long graphene strip with parallel edges is understood under the term *nanoribbon*. It can be produced by cutting the sheet of graphene. We assume the ideal case where the nanoribbon is infinitely long in one direction. There are various orientations of edges. As can be seen in Fig. 5.1, there exist two basic types of edges. One of them is the *armchair* (AC) edge. The other is called the *zigzag* (ZZ) edge.

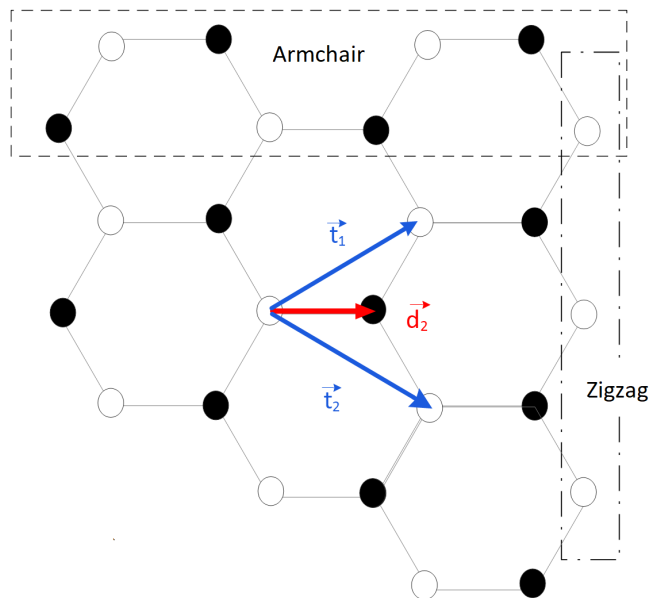


Figure 5.1: The most significant edges in nanoribbons - zigzag and armchair.

5.1 Armchair and zigzag boundary

The Hamiltonian H , which describes electrons in nanoribbons, is (4.50). The letters A, B distinguish sublattices (see 4.2) and K, K' Dirac points. H for the free Dirac fermion in the nanoribbon is

$$H = -i\sigma_0 \otimes (\sigma_1 \partial_x + \sigma_2 \partial_y), \quad \Omega = \{(x, y) \in \mathbb{R}^2 | x \in [0, L], y \in \mathbb{R}\} \quad (5.1)$$

$$\Psi = (\Psi_K, \Psi_{K'})^T \equiv (\Psi_{AK}, \Psi_{BK}, \Psi_{BK'}, \Psi_{AK'})^T.$$

The nanoribbon has a finite length L in x direction. Due to $[H, \hat{P}_y] = 0$, k_y is preserved and the bispinor Ψ is also the eigenstate of $\hat{P}_y = -i\partial_y$. We have $\hat{P}_y \Psi = k_y \Psi$. Separability of (5.1) enables us to factorize variables x, y of $\Psi(x, y)$ as

$$\Psi(x, y) = e^{ik_y y} \psi(x) = e^{ik_y y} (\psi_{AK}(x), \psi_{BK}(x), \psi_{BK'}(x), \psi_{AK'}(x))^T. \quad (5.2)$$

After the separation of variables, the equation $H\Psi = E\Psi$ converts to

$$H_{k_y} \psi = \begin{pmatrix} -i\sigma_1 \partial_x + k_y \sigma_2 & 0 \\ 0 & -i\sigma_1 \partial_x + k_y \sigma_2 \end{pmatrix} \begin{pmatrix} \psi_K \\ \psi_{K'} \end{pmatrix} = E \begin{pmatrix} \psi_K \\ \psi_{K'} \end{pmatrix}. \quad (5.3)$$

Thus, $H\Psi(x, y) = E\Psi(x, y)$ is reduced to the one-dimensional (only variable x) Dirac equation $H_{k_y} \psi(x) = E\psi(x)$. A similar problem has already been solved in 3.2 where we interchange $m \leftrightarrow k_y$.

One edge of the nanoribbon is located at $x = 0$, the latter at $x = L$. We would like to describe the boundary. On the boundary, there must hold

$$\psi(x) \Big|_{x=0} = M_1 \psi(x) \Big|_{x=0}, \quad \psi(x) \Big|_{x=L} = M_2 \psi(x) \Big|_{x=L}. \quad (5.4)$$

The matrices $M_{1,2}$ are unitary and $M_{1,2}^2 = \mathbb{I}$. They should be chosen such that the normal component to the boundary of the flux $\vec{j}^{(\psi)}(x) = \psi(x)^\dagger \sigma_0 \otimes \vec{\sigma} \psi(x)$ vanishes. For $x = 0$, resp. $x = L$, the normal vector to the boundary is $\vec{n} = (-1, 0, 0)$, resp. $\vec{n} = (1, 0, 0)$. For the normal component $j_x^{(\psi)}$, it must hold $\forall \psi, j_x^{(\psi)}(0) = j_x^{(\psi)}(L) = 0$. It can be rewritten as $\{M_{1,2}, \sigma_0 \otimes \sigma_1\} = 0$. The analysis of general b.c. was done in [15]. AC and ZZ are the most frequent ones. The most general are zigzag. AC boundary conditions are equivalent to the choice

$$M_1^{(AC)} = \sigma_1 \otimes \sigma_2, \quad M_2^{(AC)} = \sigma_1 e^{i\varphi \sigma_3} \otimes \sigma_2. \quad (5.5)$$

The explicit expressions for matrices are

$$M_1^{(AC)} = \sigma_1 \otimes \sigma_2 = \begin{pmatrix} 0 & 0 & 0 & -i \\ 0 & 0 & i & 0 \\ 0 & -i & 0 & 0 \\ i & 0 & 0 & 0 \end{pmatrix}, \quad (5.6)$$

$$M_2^{(AC)} = \sigma_1 e^{i\varphi \sigma_3} \otimes \sigma_2 = \begin{pmatrix} 0 & 0 & 0 & -ie^{-i\varphi} \\ 0 & 0 & ie^{-i\varphi} & 0 \\ 0 & -ie^{i\varphi} & 0 & 0 \\ ie^{i\varphi} & 0 & 0 & 0 \end{pmatrix}.$$

When an angle $\varphi \in \left\{0, \pm \frac{2\pi}{3}\right\}$, it expresses the width of nanoribbon. As we can find in [15], [16], $\varphi = 0 \iff L = 3pa_0$, $\varphi = \pm \frac{2\pi}{3} \iff L = (3p \pm 1)a_0$, where a_0 is the primitive vector length and $p \in \mathbb{N}$. The phase π can simulate some additional effects at the boundary. The ZZ edges have an interesting property. At the edge, the atoms of different sublattices do not mix, see Fig. 5.1. One border is made up of only white/black circles. Naturally, we would prescribe that the bispinor componets for a specific sublattice vanish at the boundary. Mathematically, it can be expressed as [15]

$$M_1^{(ZZ)} = -\sigma_3 \otimes \sigma_3, \quad M_2^{(ZZ)} = \sigma_3 \otimes \sigma_3. \quad (5.7)$$

It is worth mentioning that $[M_{1,2}^{(AC)}, \hat{\mathcal{T}}] = [M_{1,2}^{(ZZ)}, \hat{\mathcal{T}}] = 0$.

5.2 Projector method

In [17], the authors discuss a method how to effectively find functions that satisfy a specific b.c. We start with the observation that

$$[H_{k_y}, \mathbb{I} + \hat{\mathcal{P}}_x M_1] = 0, \quad M_1 = M_1^{(AC)}, \quad M_2 = M_2^{(AC)}, \quad (5.8)$$

see (5.3), where $\hat{\mathcal{P}}_x$ is the parity operator. Let us say that we know an arbitrary eigenstate $\psi(x)$ of H_{k_y} . We construct

$$\phi(x) = (\mathbb{I} + \hat{\mathcal{P}}_x M_1)\psi(x), \quad H_{k_y}\psi(x) = E\psi(x). \quad (5.9)$$

Thanks to (5.8), $\phi(x)$ is the eigenfunction of H_{k_y} . The operator $\mathbb{I} + \hat{\mathcal{P}}_x M_1$ works as a projector to the states that satisfy b.c. at $x = 0$. It can be shown in the following way. We look at $(\mathbb{I} - M_1)\phi(x) = (\mathbb{I} - M_1)(\mathbb{I}\psi(x) + M_1\psi(-x)) = (\mathbb{I} - M_1)(\psi(x) - \psi(-x))$. When we evaluate the expression at $x = 0$, we come to $(\mathbb{I} - M_1)\phi(x)\Big|_{x=0} = 0$. It implies that the first equation in (5.4) is satisfied. Thus, we obtain the solution candidate $\phi(x)$. However, $\phi(x)$ must also satisfy b.c. in the point L . After some manipulation, we get $0 = (\mathbb{I} - M_2)\phi(x)\Big|_{x=L} = (1 - M_2)[\psi(L) - M_2 M_1 \psi(-L)]$. It tells us that whenever ψ has the property $M_2 \psi(L) = M_1 \psi(-L)$, then ϕ automatically satisfies b.c. We come to the following implication

$$\begin{aligned} & \left[H_{k_y} \psi(x) = E\psi(x) \wedge [H_{k_y}, \hat{\mathcal{P}}_x M_1] = 0 \wedge M_2 \psi(L) = M_1 \psi(-L) \right] \implies \\ & \left[\phi(x) = (\mathbb{I} + \hat{\mathcal{P}}_x M_1)\psi(x), H_{k_y} \phi(x) = E\phi(x) \wedge (\mathbb{I} - M_1)\phi(0) = (\mathbb{I} - M_2)\phi(L) = 0 \right]. \end{aligned} \quad (5.10)$$

For the eigenfunctions of H_{k_y} , we prescribe armchair b.c. $M_1^{(AC)} = M_1$, $M_2^{(AC)} = M_2$, see (5.5). The projector method can be straightforwardly extended to H in (4.51). The

prerequisite is $[H, \hat{\mathcal{P}}_x M_1^{(AC)}] = 0$. The part $H_{k_y} = \sigma_0 \otimes H_K$ of H commutes trivially, see (5.8). Additionally, there must be satisfied

$$\left[\begin{pmatrix} V_K(x) & 0 \\ 0 & V_{K'}(x) \end{pmatrix}, \hat{\mathcal{P}}_x M_1^{(AC)} \right] = 0. \quad (5.11)$$

We investigate the interactions (4.53), (4.54). One can check that the commutator (5.11) is zero if and only if $A_y(x)$ is an even function,

$$[A_y(x), \hat{\mathcal{P}}_x M_1^{(AC)}] = 0 \iff A_y(x) = A_y(-x). \quad (5.12)$$

When we do the same with $\tilde{A}(x)$, we come to

$$[\tilde{A}_y(x), \hat{\mathcal{P}}_x M_1^{(AC)}] = 0 \iff \tilde{A}_y(x) = -\tilde{A}_y(-x). \quad (5.13)$$

And the mass term must be even too,

$$[M(x), \hat{\mathcal{P}}_x M_1^{(AC)}] = 0 \iff M(x) = M(-x). \quad (5.14)$$

When $A_y(x)$, $\tilde{A}_y(x)$ or $M(x)$ satisfy (5.12), (5.13) or (5.14), respectively, the projector method can be applied. It effectively transforms the task of satisfying b.c. at $x = 0$ and $x = L$ to the condition $M_2\psi(L) = M_1\psi(-L)$, see (5.10).

5.3 Additional constant mass term in Dirac Hamiltonians

We begin with two Dirac Hamiltonians $H_0 = -i\sigma_1\partial_x + V_0(x)\sigma_2$, $H = H_0 + m\sigma_3$, $m \in \mathbb{R}$. As was shown in [27], H_0 and H are from the spectral point of view in a close relationship. They are *spectrally isomorphic*. The spectral isomorphism means that there exists a real-valued function f such that $\lambda \in \sigma(H_0) \iff E = f(\lambda) \in \sigma(H)$. Let us define two component wavefunctions $\Psi_0 = (\psi_0, \xi_0)^T$, $\Psi = (\psi, \xi)^T$. The spectral isomorphism of H_0 , H can be seen from the decoupling of $H_0\Psi_0 = \lambda\Psi_0$, $\lambda \neq 0$,

$$(-\partial_x^2 + V_0' + V_0^2)\psi_0 = \lambda^2\psi_0, \quad \xi_0 = i\frac{-\psi_0' + V_0\psi_0}{\lambda} \quad (5.15)$$

and $H\Psi = E\Psi$, $E^2 \neq m^2$,

$$(-\partial_x^2 + V_0' + V_0^2)\psi = (E^2 - m^2)\psi, \quad \xi = i\frac{-\psi' + V_0\psi}{E + m}. \quad (5.16)$$

The functions ψ , ψ_0 are the eigenfunctions for different eigenvalues of the Schrödinger operator $\mathcal{H}_0^2 = -\partial_x^2 + V_0' + V_0^2$. By choice $E^2 = \lambda^2 + m^2$, we can identify $\Psi_0 \equiv \Psi$ because they have to solve the same equation. Afterwards, we rescale ξ_0 and come to

$$\frac{\lambda}{\pm|E| + m}\xi_0 = \pm i\frac{-\psi_0' + V_0\psi_0}{\sqrt{\lambda^2 + m^2} \pm m}, \quad \xi = \pm i\frac{-\psi' + V_0\psi}{\sqrt{\lambda^2 + m^2} \pm m}. \quad (5.17)$$

The plus-minus sign stands for $E \gtrless 0$. The eigenfunctions of H have changed the relative coefficients of the components compared to those of H_0 . Supplementing H_0 with a constant mass term $m\sigma_3$ does not spoil its solvability. Summarizing all the substantial formulas for $\lambda \neq 0$, we have

$$H_0\Psi_0 = \lambda\Psi_0, \quad H\Psi = E\Psi, \quad \Psi = \begin{pmatrix} 1 & 0 \\ 0 & \frac{|\lambda|}{|E| \pm m} \end{pmatrix} \Psi_0, \quad E = \pm\sqrt{\lambda^2 + m^2}. \quad (5.18)$$

Zero modes ($\lambda = 0$) for H_0 can be found in [27] as follows

$$\Psi_{0+} = \begin{pmatrix} e^{\int_0^x V_0(t) dt} \\ 0 \end{pmatrix}, \quad \Psi_{0-} = \begin{pmatrix} 0 \\ e^{-\int_0^x V_0(t) dt} \end{pmatrix}. \quad (5.19)$$

The zero modes for H_0 ($\lambda = 0$) are connected with $E = \pm m$ for H . With the aid of [27], the eigenstates are

$$\begin{aligned} E = m : \quad \Psi_+ &= \begin{pmatrix} 2C_1mie^{\int_0^x V_0(t) dt} \int_0^x e^{-2\int_0^s V_0(t) dt} ds + C_2e^{\int_0^x V_0(t) dt} \\ C_1e^{-\int_0^x V_0(t) dt} \end{pmatrix} \\ E = -m : \quad \Psi_- &= \begin{pmatrix} C_1e^{\int_0^x V_0(t) dt} \\ -2C_1Mie^{-\int_0^x V_0(t) dt} \int_0^x e^{2\int_0^s V_0(t) dt} ds + C_2e^{-\int_0^x V_0(t) dt} \end{pmatrix} \end{aligned} \quad (5.20)$$

Mapping between $\sigma(H_0)$ and $f(\sigma(H_0)) = \sigma(H)$ is provided by

$$f : \pm|\lambda| \mapsto \begin{cases} \pm\sqrt{\lambda^2 + m^2}, & \lambda \neq 0 \\ -m \text{ or } m, & \lambda = 0. \end{cases} \quad (5.21)$$

5.4 Strained nanoribbons

In 4.6.1 we show that a pseudo-magnetic field in the nanoribbon can be caused by the strain field. It is defined in (4.57). Let us take the pseudo-vector potential $\tilde{A}_y(x)$ as follows

$$\tilde{A}_y(x) = -\frac{2\beta}{a}u_{12}(x) = -\frac{\beta}{a\mu}\sigma_{12}(x) = K_0\text{tgh}(K_0x), \quad x \in [0, L], \quad (5.22)$$

where we used (4.56). Shear stress is a monotonous function with $\sigma_{12}(0) = 0$. Returning back to (4.55), we have to solve the differential equation for the unknown displacement $\vec{u} = (u_1(x), u_2(x))$. Assumption $u_1 \approx 0$ gives

$$-\frac{aK_0}{2\beta}\text{tgh}(K_0x) = \frac{1}{2}\partial_x u_2(x). \quad (5.23)$$

The displacement of carbon atoms on the y axis is

$$u_2(x) = -\frac{a}{\beta} \ln(\text{ch}(K_0x)) + C, \quad C \in \mathbb{R}. \quad (5.24)$$

At $(x, y) = (0, y)$, the nanoribbon is not affected by shear. Atoms with the coordinate $x = 0$ remain at their original positions. Therefore, $u_2(0) = 0 \Rightarrow C \equiv 0$. The result is that the atoms are displaced from their original location x_0, y_0 to

$$\begin{aligned} x &= x_0 + u_1 \approx x_0 \\ y &= y_0 + u_2 \approx y_0 - \frac{a}{\beta} \ln(\text{ch}(K_0x_0)). \end{aligned} \quad (5.25)$$

The strained nanoribbon is depicted in Fig. 5.2. In this way deformed nanoribbons, it is induced an effective pseudo-magnetic field

$$B_z(x) = \partial_x \tilde{A}_y(x) = \frac{K_0^2}{\text{ch}^2(K_0x)}. \quad (5.26)$$

Several remarks are in order:

- Generally, the sign of the pseudo-magnetic field depends on the sign of $-\partial_x u_{12}(x)$, see (5.22). In our case, the sign of the pseudo-magnetic field depends on the direction of displacement. Moving atoms in the opposite direction than in Fig. 5.2, we can control the sign of $B_z(x)$.
- The pseudo-magnetic field has an extreme value for $x = 0$. We considered the location of the nanoribbon $x \in [0, L]$. The situation can be generalized to $[-L, L]$, when we obtain a pseudo-magnetic field focused in the center of the nanoribbon.
- The strength of the pseudo-magnetic field is impressive. For different a configuration of the graphene sheet, authors of [5] state $B_z \approx 10$ T. It could be expected that our generated field would have similar strength.

5.5 Formal model of strained nanoribbons

The model of a strained nanoribbon will be described by the 2D Hamiltonian

$$H_{k_y} = -i\sigma_0 \otimes \sigma_1 \partial_x + k_y \sigma_0 \otimes \sigma_2 + \sigma_3 \otimes \sigma_2 K_0 \text{tgh}(K_0x). \quad (5.27)$$

If we fix $k_y = 0$, we obtain

$$H = \begin{pmatrix} H_2 & 0 \\ 0 & \sigma_1 H_2 \sigma_1 \end{pmatrix} = -i\sigma_0 \otimes \sigma_1 \partial_x + \sigma_3 \otimes \sigma_2 K_0 \text{tgh}(K_0x), \quad K_0 = |m| > 0. \quad (5.28)$$

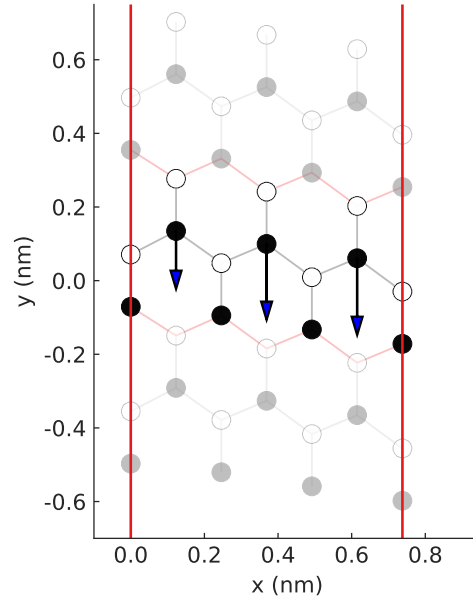


Figure 5.2: The AC nanoribbon under the influence of strain field (5.22). The width of nanoribbon is $3a_0 \doteq 0.737$ nm. The arrows represent shear stress. Parameters are $\beta = 3$, $K_0 = 6.708$. The shaded region indicates translation symmetry in y .

H contains solvable H_2 for $\varepsilon = 0$, which was discussed in (3.26). We look at the eigenvalue equation $H\psi = E\psi$. This has been the content of 3.2.1, especially the formulas in (3.26). The wavefunctions of H are

$$\psi = \begin{pmatrix} \psi'_{AK} - im\psi_{BK} \\ \psi'_{BK} - K_0 \operatorname{tgh}(K_0 x) \psi_{BK} \\ \psi'_{AK'} - K_0 \operatorname{tgh}(K_0 x) \psi_{AK'} \\ \psi'_{BK'} - im\psi_{AK'} \end{pmatrix}. \quad (5.29)$$

Here, $\psi_{AK,AK'}$ and $\psi_{BK,BK'}$ are

$$\begin{pmatrix} \psi_{AK} \\ \psi_{BK} \end{pmatrix} = C_{1K} e^{ikx} \begin{pmatrix} 1 \\ k \\ E+m \end{pmatrix} + C_{2K} e^{-ikx} \begin{pmatrix} 1 \\ -k \\ -E+m \end{pmatrix}, \quad k = \sqrt{E^2 - m^2} \in \mathbb{C}, \quad (5.30)$$

$$\begin{pmatrix} \psi_{BK'} \\ \psi_{AK'} \end{pmatrix} = C_{1K'} e^{ikx} \begin{pmatrix} 1 \\ k \\ E+m \end{pmatrix} + C_{2K'} e^{-ikx} \begin{pmatrix} 1 \\ -k \\ -E+m \end{pmatrix}, \quad C_{1K'}, C_{2K'} \in \mathbb{C}.$$

The missing states v_2, \tilde{v}_2 for $E = \varepsilon = 0$ are (see (3.26) and (3.14))

$$v_2 = \left(0, \frac{1}{\operatorname{ch}(K_0 x)}, \frac{1}{\operatorname{ch}(K_0 x)}, 0 \right)^T, \quad \tilde{v}_2 = (\operatorname{ch}(K_0 x), 0, 0, \operatorname{ch}(K_0 x))^T. \quad (5.31)$$

The missing states for $E = m$ are

$$v_1 = \begin{pmatrix} 1 \\ i \operatorname{tgh}(K_0 x) \\ i \operatorname{tgh}(K_0 x) \\ 1 \end{pmatrix}, \quad \tilde{v}_1 = \begin{pmatrix} -imx \\ mxt \operatorname{tgh}(K_0 x) - 1 \\ mxt \operatorname{tgh}(K_0 x) - 1 \\ -imx \end{pmatrix}. \quad (5.32)$$

5.5.1 Strained armchair nanoribbon

Our purpose is to find a solution of (5.28), which will be compatible with the AC b.c. given by $M_1 = M_1^{(AC)} = \sigma_1 \otimes \sigma_2$, $M_2 = M_2^{(AC)} = \sigma_1 e^{i\varphi\sigma_3} \otimes \sigma_2$. The Hamiltonian H satisfies $[H, \hat{P}_x M_1] = 0$, because of (5.13). We can utilize the projector method 5.2. It converts the boundary condition at $x = 0$ and $x = L$ into the following single auxiliary condition

$$M_1 \psi(-L) = \sigma_1 \otimes \sigma_2 \psi(-L) = \sigma_1 e^{i\varphi\sigma_3} \otimes \sigma_2 \psi(L) = M_2 \psi(L). \quad (5.33)$$

This is a system of linear equations, the unknowns are C_{1K} , C_{2K} , $C_{2K'}$, $C_{1K'}$ and E . We remind that $M_{1,2}$ are anti-diagonal. Thus, the components of ψ in (5.33) do not mix together. For example, one equation of the system is $ie^{i\varphi}(1, 0, 0, 0)\psi(L) = i(1, 0, 0, 0)\psi(-L)$. In each equation, there are either coefficients C_{1K} , C_{2K} or $C_{2K'}$, $C_{1K'}$ but not all four together. Thus the system of linear equations (5.33) takes the form

$$\left(\begin{array}{cc|cc} \mathbb{B}(\varphi) & 0 & 0 & \\ \hline & 0 & 0 & \\ 0 & 0 & \mathbb{B}(-\varphi) & \\ 0 & 0 & & \end{array} \right) \begin{pmatrix} C_{1K} \\ C_{2K} \\ C_{1K'} \\ C_{2K'} \end{pmatrix} = \vec{0}. \quad (5.34)$$

The block $\mathbb{B}(\varphi)$ has the form

$$\mathbb{B}(\varphi) = \begin{pmatrix} E \sin\left(kL + \frac{\varphi}{2}\right) & -E \sin\left(kL - \frac{\varphi}{2}\right) \\ k \sin\left(kL + \frac{\varphi}{2}\right) + K_0 \operatorname{tgh}(K_0 L) \cos\left(kL + \frac{\varphi}{2}\right) & k \sin\left(kL - \frac{\varphi}{2}\right) + K_0 \operatorname{tgh}(K_0 L) \cos\left(kL - \frac{\varphi}{2}\right) \end{pmatrix}. \quad (5.35)$$

The variables are $k = \sqrt{E^2 - m^2}$, $K_0 = |m|$. The spectrum of (5.28) is obtained by calculating the values of k where the determinant equals zero, which is the product $\det\{\mathbb{B}(\varphi)\} \det\{\mathbb{B}(-\varphi)\} = 0$. Apparently, we seek for solutions of the following equation

$$\det(\mathbb{B}(\pm\varphi)) = E [k (\cos(\varphi) - \cos(2kL)) + K_0 \operatorname{tgh}(K_0 L) \sin(2kL)] \stackrel{!}{=} 0. \quad (5.36)$$

We immediately see the solution $E = 0$ or $E = \pm m$. Unfortunately, these are the missing and degenerated states and they should be treated in a different way. Let us then leave until later. Expression in (5.36) gives rise to energy levels that have to be found numerically. Generally, we expect countable infinite solutions $k \in \mathbb{R}$. This is due to two oscillating functions, where one of them has a modulated amplitude by k . The coefficients $C_{jK^{(\prime)}}$ can be obtained from (5.35) and (5.34).

The states with $E = \varepsilon = 0$ are given by (5.31). It holds $M_1 v_2(L) = M_2 v_2(-L) \iff \varphi = 0$ and $M_1 \tilde{v}_2(L) = M_2 \tilde{v}_2(-L) \iff \varphi = 0$. Thus, $E = 0$ appears in the spectrum only for $\varphi = 0$. The eigenstates for the missing energy $E = m$ can be found in (5.32). From the condition

$$M_1 [C_1 v_1(L) + C_2 \tilde{v}_1(L)] = M_2 [C_1 v_1(-L) + C_2 \tilde{v}_1(-L)], \quad C_{1,2} \in \mathbb{C}, \quad (5.37)$$

we get the relation between φ and parameters m , L

$$0 < mL \operatorname{tgh}(K_0 L) = mL \operatorname{tgh}(mL) = \sin^2\left(\frac{\varphi}{2}\right). \quad (5.38)$$

The energy $E = m$ appears for special setup of parameters m , L , φ when $mL\text{tgh}(mL) \leq 1$, $\varphi \neq 0$. The chiral symmetry $S = \sigma_3 \otimes \sigma_3$ of $H = -SHS$ and $[M_{1,2}, S] = 0$ dictate that $E = -m$ can be obtained via $S(C_1v_1 + C_2\tilde{v}_1)$. With this knowledge, we can determine ψ that satisfies (5.33). The real eigenstates of H are $(\mathbb{I} + \hat{\mathcal{P}}_x M_1)\psi(x)$, see (5.9). The density probability functions for different widths of AC nanoribbons are illustrated in Fig. 5.3. The majority of the density probability for both A, B components is pushed closer to $x = L$ or $x = 0$ for low energies.

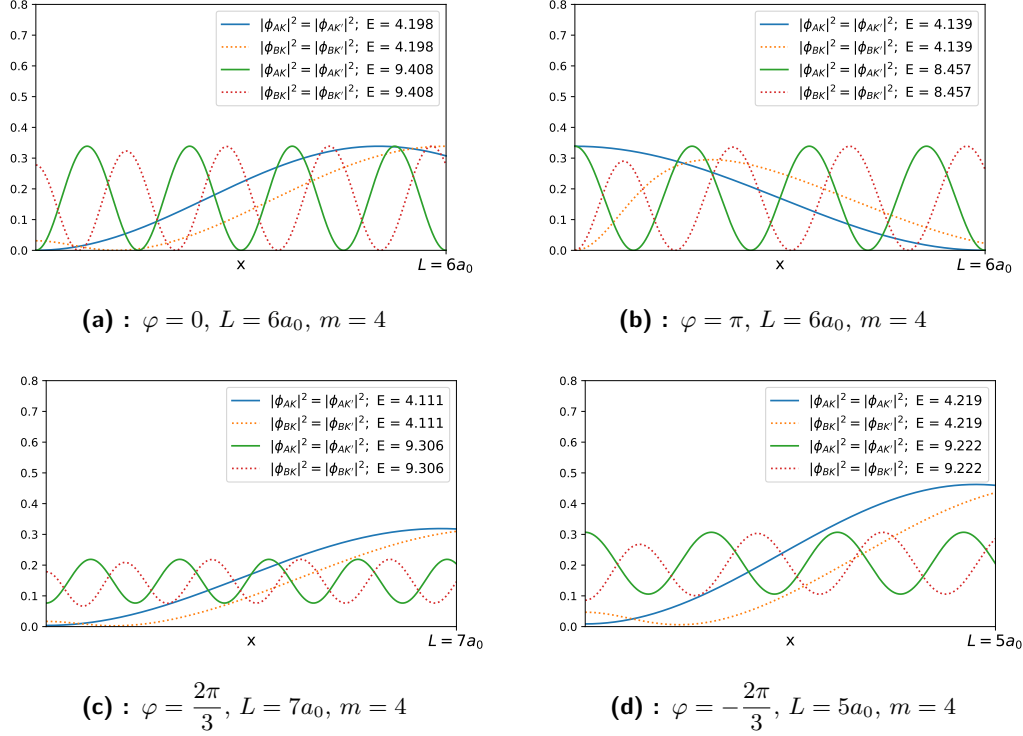


Figure 5.3: Density probability functions for metallic (a), semiconducting (c), (d) and phase π (b) strained AC nanoribbons with the Hamiltonian (5.27) for $k_y = 0$. The functions ϕ_{AK} , $\phi_{AK'}$, ϕ_{BK} , $\phi_{BK'}$ are components of $\Phi = (\mathbb{I} + M_1 \hat{\mathcal{P}}_x)\psi(x)$, where $\psi(x)$ is given by (5.29). The parameter $a_0 = 0.142\sqrt{3}$ is the length of primitive translation vector.

5.5.2 Strained zigzag nanoribbon

We take again (5.28) and prescribe ZZ b.c. given by (5.7). They imply

$$\psi_{AK}(0) = 0, \quad \psi_{AK'}(0) = 0, \quad \psi_{BK}(L) = 0, \quad \psi_{BK'}(L) = 0. \quad (5.39)$$

We begin with zero modes given by (5.31). It is evident that they do not satisfy ZZ b.c. and $E = 0$ does not appear in the spectrum. For states with $E = m$ in (5.32), it is relevant

only \tilde{v}_1 due to $\alpha v_{1AK}(0) + \tilde{v}_{1AK}(0) = \alpha v_{1AK}(0) = 0 \iff \alpha = 0$. Thus, energy $E = \pm m$ is present in the spectrum when

$$\tilde{v}_{1BK} = \tilde{v}_{1BK'} = 0 \iff mL \operatorname{tgh}(K_0L) = 1. \quad (5.40)$$

It always has only one solution, which is the intersection of $\frac{1}{mL} = \operatorname{tgh}(mL)$, $mL > 0$. So for a special setup of m , L , the energies $\pm m$ appear in $\sigma(H)$. The bispinor $\psi = (\psi_{AK}, \psi_{BK}, \psi_{BK'}, \psi_{AK'})^T$ can be found in (5.29). Substituting ψ to ZZ b.c. (5.39) gives us

$$\begin{aligned} ik \left(1 - \frac{m}{P}\right) (C_{1K^{(\prime)}} + C_{2K^{(\prime)}}) &= 0 \\ \frac{ik^2}{P} (C_{1K^{(\prime)}} e^{ikL} - C_{2K^{(\prime)}} e^{-ikL}) - \frac{K_0 k}{P} \operatorname{tgh}(K_0L) (C_{1K^{(\prime)}} e^{ikL} + C_{2K^{(\prime)}} e^{-ikL}) &= 0 \end{aligned} \quad (5.41)$$

From the first equation $C_{1K} = -C_{2K}$, $C_{1K'} = -C_{2K'}$. Substituting the constants to the latter equation, we obtain a condition

$$\frac{k}{K_0} = \operatorname{tgh}(K_0L) \operatorname{tg}(kL), \quad k^2 = E^2 - m^2, \quad K_0 = m. \quad (5.42)$$

The exact value of k must be calculated numerically. We have found the relation between $C_{1K^{(\prime)}}$, $C_{2K^{(\prime)}}$ below (5.41). The energy spectrum of H is based on (5.42). Rewriting the complex exponentials to sines and cosines, the eigenfunctions ψ of $H\psi = E\psi$ satisfying ZZ b.c. are

$$\psi = \mathcal{N} \begin{pmatrix} -E \sin(kx) \\ ik \cos(kx) - iK_0 \operatorname{tgh}(K_0x) \sin(kx) \\ ik \cos(kx) - iK_0 \operatorname{tgh}(K_0x) \sin(kx) \\ -E \sin(kx) \end{pmatrix}. \quad (5.43)$$

\mathcal{N} is a normalization constant. The density probability for the components of ψ is shown in Fig. 5.4. In contrast with Fig. 5.3, the density probability is centered more in the middle of nanoribbons.

5.6 2D Dirac operator hidden in 1D Dirac operator

Let us suppose that we apply DT on the effective 1D operator $H_{k_{0y}} = -i\sigma_1 \partial_x + \sigma_2 k_{0y}$ and create H . Generally, the interaction in the new transformed system will depend on k_{0y} , that is $H = -i\sigma_1 \partial_x + \sigma_2 k_{0y} + V(x, k_{0y})$. If we fix different value of the momentum k_y then $H_{k_y} = -i\sigma_1 \partial_x + \sigma_2 k_y + V(x, k_{0y})$. But it can be hard to find the eigenstates of H_{k_y} . The knowledge of the eigenstates of $H_{k_{0y}}$ is not helpful in general.

Let us consider the 1D Dirac Hamiltonian H_0 with an arbitrary mass term $M(x)$

$$H_0 = -i\sigma_0 \otimes \sigma_1 \partial_x + M(x) \sigma_3 \otimes \sigma_3. \quad (5.44)$$

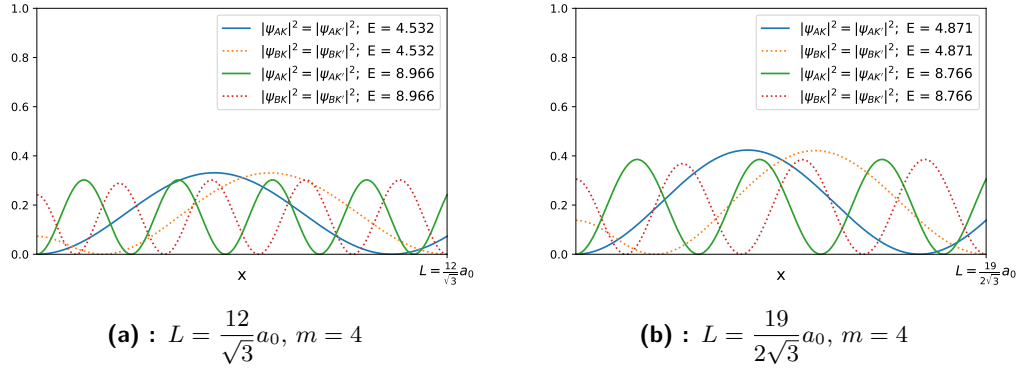


Figure 5.4: Density probability functions for strained ZZ nanoribbons. The components $\psi_A, \psi_B, \psi_{B'}, \psi_{A'}$ belong to ψ given by (5.43). Parameter $a_0 = 0.142\sqrt{3}$.

We show that the solvability of H_0 gives the opportunity to explicitly find eigenstates of the two-dimensional H ,

$$H = -i\sigma_0 \otimes \sigma_1 \partial_x + k_y \sigma_0 \otimes \sigma_2 + M(x) \sigma_3 \otimes \sigma_3. \quad (5.45)$$

We assume that H_0 is solvable. First, H_0 can be converted to

$$U_1 H_0 U_1^\dagger = \begin{pmatrix} \sigma_0 & 0 \\ 0 & \sigma_1 \end{pmatrix} H_0 \begin{pmatrix} \sigma_0 & 0 \\ 0 & \sigma_1 \end{pmatrix} = -i\sigma_0 \otimes \sigma_1 \partial_x + M(x) \sigma_0 \otimes \sigma_3. \quad (5.46)$$

Another unitary transformation $U_2 = \sigma_0 \otimes e^{-i\frac{\pi}{4}\sigma_1}$ brings $U_1 H_0 U_1^\dagger$ to

$$\tilde{H}_0 = U_2 U_1 H_0 U_1^\dagger U_2^\dagger = -i\sigma_0 \otimes \sigma_1 \partial_x - M(x) \sigma_0 \otimes \sigma_2. \quad (5.47)$$

We add the additional term $k_y \sigma_3 \otimes \sigma_3$ to \tilde{H}_0 . So we construct

$$\tilde{H} = \tilde{H}_0 + k_y \sigma_3 \otimes \sigma_3 \quad (5.48)$$

and use the fact that the addition of $k_y \sigma_3 \otimes \sigma_3$ does not spoil the solvability, see 5.3, for arbitrary k_y . In other words, we can find the eigenstates of \tilde{H} from the eigenstates of \tilde{H}_0 . In the last step, we return back to H_0 in the following way

$$H = U_1^\dagger U_2^\dagger \tilde{H} U_2 U_1 = U_1^\dagger U_2^\dagger \tilde{H}_0 U_2 U_1 + k_y U_1^\dagger U_2^\dagger \sigma_3 \otimes \sigma_3 U_2 U_1 = H_0 + k_y \sigma_0 \otimes \sigma_2. \quad (5.49)$$

H_0 can be transformed to H by a chain of unitary transformations and by addition of the term $k_y \sigma_3 \otimes \sigma_3$. The eigenstates Ψ of H can be obtained from the eigenstates Ψ_0 of H_0 by the operator \mathbb{U} such that

$$\Psi = \mathbb{U} \Psi_0, \quad \mathbb{U} = U_1^\dagger U_2^\dagger D U_2 U_1, \quad D = \begin{pmatrix} 1 & 0 & 0 & 0 \\ 0 & \frac{|\lambda|}{\sqrt{\lambda^2 + k_y^2} \pm k_y} & 0 & 0 \\ 0 & 0 & 1 & 0 \\ 0 & 0 & 0 & \frac{|\lambda|}{\sqrt{\lambda^2 + k_y^2} \mp k_y} \end{pmatrix}. \quad (5.50)$$

The most important thing is that we move from a 1D on to a 2D problem,

$$\begin{aligned} H &= -i\sigma_0 \otimes (\sigma_1 \partial_x + \sigma_2 \partial_y) + M(x)\sigma_3 \otimes \sigma_3, \\ H \left(e^{ik_y y} \Phi(x) \right) &= E e^{ik_y y} \Phi(x). \end{aligned} \quad (5.51)$$

By construction, the momentum k_y is arbitrary. We realize that the final potential remains the same for all k_y .

5.7 AC nanoribbon in staggered field

Using the results of 5.6, we choose $M(x)$ and construct H_0 as

$$H_0 = \begin{pmatrix} H_2 & 0 \\ 0 & \sigma_1 H_2 \sigma_1 \end{pmatrix} = -i\sigma_0 \otimes \sigma_1 \partial_x + \left(m - \frac{K_\varepsilon^2}{m + \varepsilon \operatorname{ch}(2K_\varepsilon x)} \right) \sigma_3 \otimes \sigma_3. \quad (5.52)$$

The parameter $m > 0$ is arbitrary, $\varepsilon \in (0, m)$ and x is from the finite interval $x \in [0, L]$. The solvability of H_2 discussed in 3.2.2 is inherited by H_0 . So, we know the eigenstates Ψ_0 of H_0 and $\lambda \in \sigma(H_0)$. Extension of H_0 to 2D is

$$H = -i\sigma_0 \otimes (\sigma_1 \partial_x + \sigma_2 \partial_y) + \left(m - \frac{K_\varepsilon^2}{m + \varepsilon \operatorname{ch}(2K_\varepsilon x)} \right) \sigma_3 \otimes \sigma_3. \quad (5.53)$$

The eigenfunctions of H are considered in a form $e^{ik_y y} \Psi(x)$. The Hamiltonian describes a model of nanoribbon in a staggered field, which is visualized in Fig. 5.5.

We will focus on the AC b.c. given by (5.5). We shall find the spectrum and the eigenfunctions of H , i.e. we shall solve $H e^{ik_y y} \Psi = E e^{ik_y y} \Psi$. The potential $M(x)$ is an even function. It fits like a glove on (5.14). So, we can find $\sigma(H)$ and Ψ through the projector method mentioned in 5.2. The calculation is based on the fulfillment of $M_1 e^{ik_y y} \Psi(-L) = M_2 e^{ik_y y} \Psi(L)$, see (5.10). On both sides, the exponentials $e^{ik_y y}$ cancel out. We do not have to forget that Ψ is transformed Ψ_0 . The relation between them is ($\lambda \in \mathbb{R} \setminus \{\pm\varepsilon, 0\}$)

$$\Psi = \mathbb{U} \Psi_0 = U_1^\dagger U_2^\dagger D U_2 U_1 \Psi_0. \quad (5.54)$$

The matrix \mathbb{U} can be found in (5.50). The matrix D brings dependence on k_y of the wavefunctions Ψ . Initially simple $M_1 \Psi(-L) = M_2 \Psi(L)$ gets complicated a lot. It can be driven to the following secular equation where the explicit dependence on k_y cancels out,

$$\begin{aligned}
 & \left[\xi_1 \sin \left(kL - \frac{\varphi}{2} \right) + \xi_2 \cos \left(kL - \frac{\varphi}{2} \right) \right] \left[\xi_3 \sin \left(kL + \frac{\varphi}{2} \right) - \xi \cos \left(kL + \frac{\varphi}{2} \right) \right] + \\
 & + \left[\xi_3 \sin \left(kL - \frac{\varphi}{2} \right) - \xi \cos \left(kL - \frac{\varphi}{2} \right) \right] \left[\xi_1 \sin \left(kL + \frac{\varphi}{2} \right) + \xi_2 \cos \left(kL + \frac{\varphi}{2} \right) \right] = 0, \text{ where} \\
 & \xi = \frac{\varepsilon K_\varepsilon \text{sh}(2K_\varepsilon L)}{m + \varepsilon \text{ch}(2K_\varepsilon L)}, \quad \xi_1 = \lambda - m + \frac{K_\varepsilon^2}{m + \varepsilon \text{ch}(2K_\varepsilon L)}, \\
 & \xi_2 = \xi \frac{k}{\lambda + m}, \quad \xi_3 = -k + \frac{k K_\varepsilon^2}{(\lambda + m)(m + \varepsilon \text{ch}(2K_\varepsilon L))}.
 \end{aligned} \tag{5.55}$$

Let us remind that $k = \sqrt{\lambda^2 - m^2}$, $K_\varepsilon = \sqrt{m^2 - \varepsilon^2}$. Auxiliary energy λ is determined by zeros of the secular equation. The energy spectrum of H is the set of energies $\sigma(H) = \{E \in \mathbb{R} | E^2 = \lambda^2 + k_y^2, k_y \in \mathbb{R}\}$, where lambdas are solutions (5.55). For high energies ($\lambda \gg m$), λ is determined by $\sin \left(kL \pm \frac{\varphi}{2} \right) = 0$. It can be seen from (5.55) where we leave terms of dominant order λ .

Energies $\lambda^2 < m^2$ are not solutions of the secular equation (5.55), except $\lambda = \pm \varepsilon$. This fact is not evident from the first look at the secular equation. When we use the sine and cosine formula for the sum of arguments and rewrite $\sin(kL)$, $\cos(kL)$, $k = \sqrt{\lambda^2 - m^2}$ as $\text{ish}(KL)$, $\text{ch}(KL)$, $k = i\sqrt{m^2 - \lambda^2} = iK$, the numerical solution of the secular equation are only the missing energies $\lambda = \pm \varepsilon$. However, $\lambda = \pm \varepsilon$ are not relevant, because the missing states must be treated differently and we assumed $\lambda \neq \pm \varepsilon$. The missing states v_1, v_2 from (3.29) do not satisfy $M_1 U v_{1,2}(-L) = M_2 U v_{1,2}(L)$. Finding of the second linearly independent solutions \tilde{v}_1, \tilde{v}_2 through (3.14) is extremely complicated. So, we have not

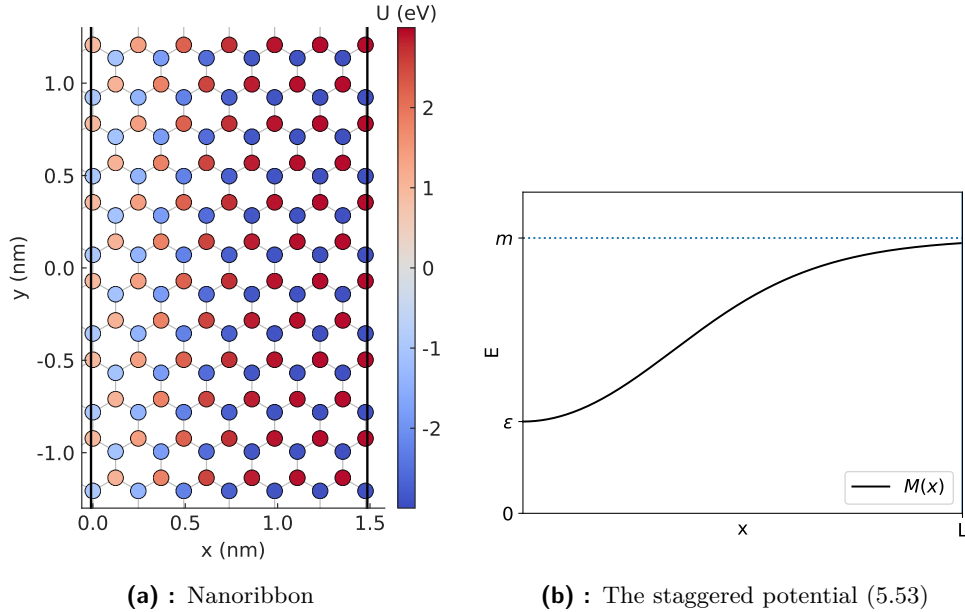


Figure 5.5: Nanoribbon in staggered potential $M(x)$ given by (5.53) for $L = 1.5$, $m = 3$, $\varepsilon = 1$. The length in y is infinite and in x finite.

archived the conclusive result whether $\pm\varepsilon$ is in $\sigma(H)$. We took out also $\lambda = 0$. The zero modes with $\lambda = 0$ of H_0 are related to $E = \pm k_y$ for H . We take the zero modes Ψ_{\pm} of (5.48) which have the form (5.20). We transform them by $U_1^\dagger U_2^\dagger$ and we look at $M_1 U_1^\dagger U_2^\dagger \Psi_{\pm}(-L) = M_2 U_1^\dagger U_2^\dagger \Psi_{\pm}(L)$. The AC b.c. matrices (5.5) enforce that $U_1^\dagger U_2^\dagger \Psi_{\pm} = \vec{0}$ for all angles φ . Thus, the energy $E = \pm k_y$ cannot appear in $\sigma(H)$.

Let us denote $\Phi(x) = (\Phi_A(x), \Phi_B(x), \Phi_{B'}(x), \Phi_{A'}(x))$. The eigenfunctions $e^{ik_y y} \Phi(x)$ of H , which satisfy b.c., are constructed by the projection of $e^{ik_y y} \Psi(x)$, see (5.10). They are obtained from $e^{ik_y y} \Phi = e^{ik_y y} (\mathbb{I} + \hat{\mathcal{P}}_x M_1) \Psi = e^{ik_y y} (\mathbb{I} + \hat{\mathcal{P}}_x M_1) U \Psi_0$. Density probability functions $|\Phi_{A'}|^2$, $|\Phi_{B'}|^2$ in high and low energy modes for different φ are plotted in Fig. 5.7. We see that the differences between $|\Phi_A|^2$ and $|\Phi_B|^2$ almost disappear for high energies. It can be said about K' valley components too. The reason is in (5.50) where the B components are rescaled, but for high λ is $D \sim \mathbb{I}$. Also, the $|\Phi_A|^2$ and $|\Phi_{A'}|^2$ are not the same which is due to the opposite sign of k_y in (5.50). Further, when densities for A components have local minima, densities for B components reach local maxima.

Remarkably, the behavior of density probability functions strongly depends on the angle φ . This is caused by the value of constants $C_{1K'}$, $C_{2K'}$. For angles $\varphi \pm \frac{2\pi}{3}$, it is $C_{1K'} \approx 0$, $C_{2K} \approx 0$ and $C_{2K'} \gg C_{1K'}$, $C_{1K} \gg C_{2K}$. On the contrary, when $\varphi \in \{0, \pi\}$ then all $C_{iK'} \gg 0$. If we look at ψ in (3.27), only term e^{ikx} resp. e^{-ikx} remains when we set $C_2 = 0$ resp. $C_1 = 0$. From the construction of Ψ , it follows that Ψ has the form $\Psi = (f_1(x)e^{ikx}, f_2(x)e^{ikx}, f_3(x)e^{-ikx}, f_4(x)e^{-ikx})$. Functions f_i can be exactly defined, nevertheless they do not contain oscillating functions e^{ikx} or e^{-ikx} . The projector $\mathbb{I} + \mathcal{P}_x M_1$ does

$$\Phi = (\mathbb{I} + \mathcal{P}_x M_1) \Psi = \begin{pmatrix} (f_1(x) - if_4(-x))e^{ikx} \\ (f_2(x) + if_3(-x))e^{ikx} \\ (f_3(x) - if_2(-x))e^{-ikx} \\ (f_4(x) + if_1(-x))e^{-ikx} \end{pmatrix}. \quad (5.56)$$

Now, it is evident that $|\Phi_{A'}|^2$, $|\Phi_{B'}|^2$ do not oscillate. This is the case of $\varphi = \pm \frac{2\pi}{3}$. In contrast, when all the constants do not vanish, the complex exponentials set up sines and cosines right in (3.27) and $|\Phi_{A'}|^2$, $|\Phi_{B'}|^2$ are oscillating functions. As was mentioned, oscillations holds for $\varphi \in \{0, \pi\}$.

The model (5.53) and band structures are visualized in Fig. 5.5 and Fig. 5.6. From the picture it is evident that $\varepsilon \in (0, m)$ controls the inhomogeneity of potential. The band gaps ΔE are bigger for larger m . It is because of $\lambda^2 \geq m^2 \implies E^2 = \lambda^2 + k_y^2 \geq m^2 + k_y^2 \geq m^2$. So, the the lower limit of the conductive band is always greater than m and the upper limit of the valence band is smaller than $-m$. The minimal band gap can be $\Delta E = 2m$. The width of the band gap is $(\Delta E)_{met} = 2m$ for metallic AC nanoribbons. It is due to $\varphi = 0 \implies E = \pm \sqrt{m^2 + k_y^2} \in \sigma(H) \implies E = \pm m \in \sigma(H)$. Semi-conducting nanoribbons have the gap $(\Delta E)_{semi} > (\Delta E)_{met} = 2m$ because $\varphi = \pm \frac{2\pi}{3} \implies E = \pm \sqrt{m^2 + k_y^2} \notin \sigma(H) \implies E = \pm m \notin \sigma(H)$. Analogical consideration holds true for $\varphi = \pi$. The increasing width

of semi-conducting nanoribbons leads to decrease of ΔE and to higher number of lines in band structure.

The domain of x was taken as $x \in [0, L]$. Supposing the x -domain as $x \in [-L, L]$, we can get the potential as an even function of x . It might be presumed that the electrons (or their wavefunctions) would be localized in the area of smaller potential magnitude. Model would resemble a graphene waveguide. Because of the high velocity of electrons in graphene, plasmons can travel further distances than in standard mediums such as metal-dielectric. Also, it is possible to design graphene optical fibers [28]. Recently, we became aware of the experiment [29] where the authors shined with a laser on graphene sheet in staggered potential. The laser emitted light at the angular frequency ω_0 . Lit graphene then radiated at angular frequency $2\omega_0$ (the second harmonic frequency), which could find application in non-linear optics. It is worth mentioning that the experiment was carried out under drastic conditions when the sample was cooled by liquid helium.

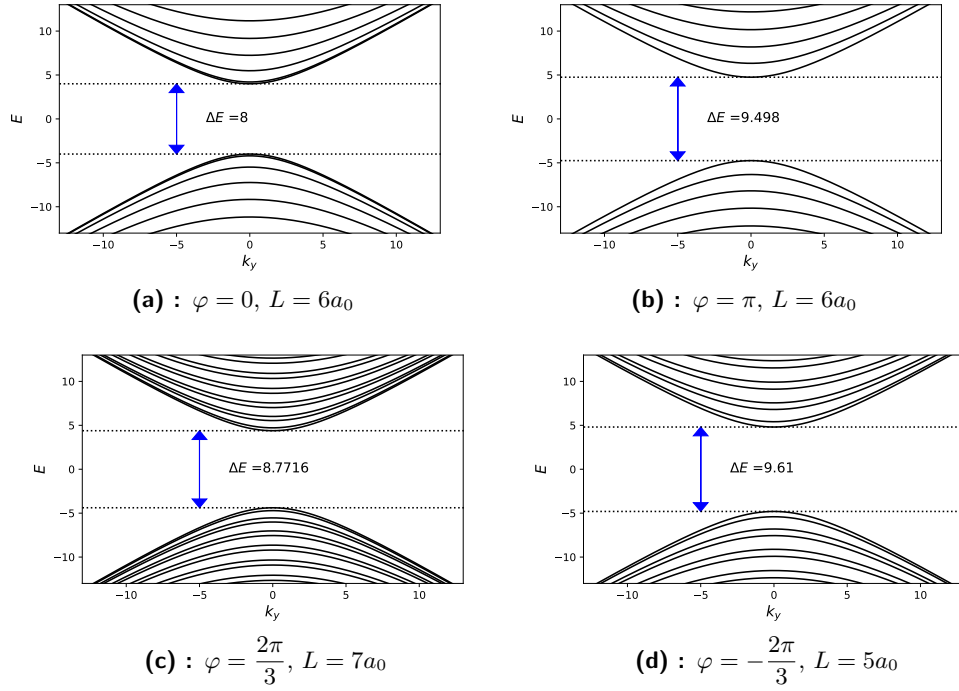


Figure 5.6: Band structures for metallic (a), (b) and semiconducting (c), (d) AC nanoribbons placed in staggered potential (5.53). The band gap in (c), (d) is wider than in (a), (b). For all figures, parameters are $a_0 = 0.142\sqrt{3}$, $m = 4$, $\varepsilon = 2$.

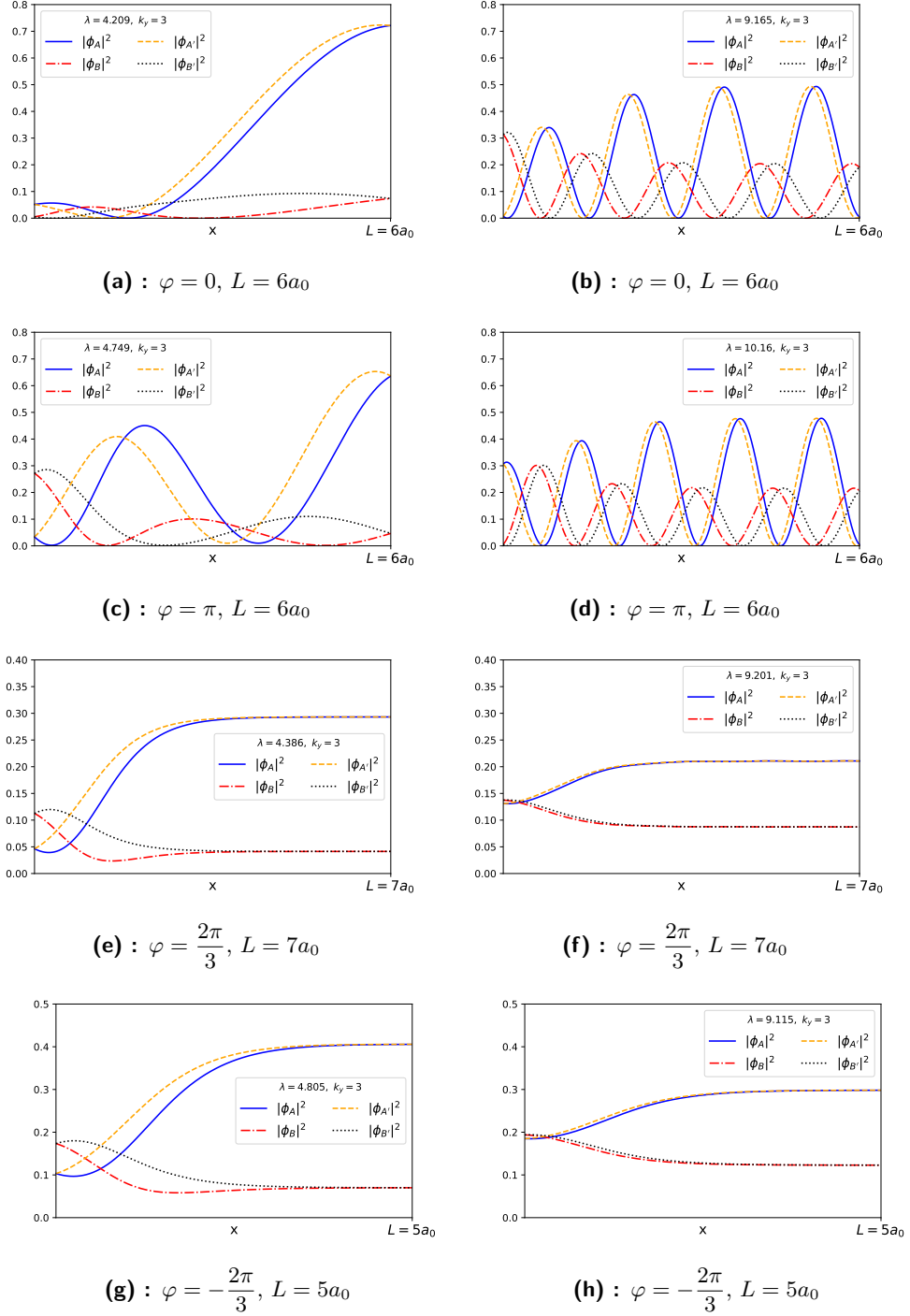


Figure 5.7: The comparison of density probability functions $|\Phi_A|^2$, $|\Phi_B|^2$, $|\Phi_{A'}|^2$, $|\Phi_{B'}|^2$ for different angles φ in low (left) and high (right) energy modes. The function Φ is the solution of $H e^{ik_y y} \Phi(x) = \sqrt{\lambda^2 + k_y^2} e^{ik_y y} \Phi(x)$ where H is given by (5.53). In the figures, we change λ which is the solution of (5.55). Parameters $a_0 = 0.142\sqrt{3}$, $k_y = 3$, $m = 4$, $\varepsilon = 2$ are the same for all figures.



Chapter 6

Conclusions

Last of all, let us summarize the results and outline the possible future improvement. In the first part of the thesis, we reviewed the DT for Schrödinger operators and its connection with SUSY QM. The transformation was formally applied to the models of infinite and finite square wells. We were able to find the spectrum in dependence on prescribed b.c. Special attention was paid to the bound states. In section 2.4 we derive general condition (2.48) for solutions of ISW, such that their DT complies with prescribed b.c. Further, the results of 2.5, 2.5.1, 2.5.2 indicate that both regular and singular potentials can be obtained via DT from the finite square well (FSW) model. The comparison of spectra in Fig. 2.5 revealed that FSW has more energy levels than both regularized wells. The potential \sec^2 in Fig. 2.3 could be employed as a better approximation of FSW with the relatively simple form of eigenfunctions, see (2.73), (2.79). The potential \csc^2 in Fig. 2.4 can be restricted to $r = x \in [0, +\infty)$ and used in spherical symmetric problems for the s states. Its form is similar to the potentials used in a chemical bonding, see [30]. With the proper setup of parameters, \csc^2 can approximate the chemical bonding potentials.

The second part of the thesis started with the review of DT for 1D Dirac operator. We applied it to the model of 1D Dirac free particle which provides us with two examples (3.26) and (3.30). In the first, an inhomogeneous parity-odd vector potential was presented, while in the latter occurred inhomogeneous parity-even mass term. Next, we summarized basic definition and terms for the description of crystals. We reviewed the tight-binding model of graphene. We observed that the electrons in graphene with momentum near the Dirac points are effectively described by 2D Dirac equation, see (4.50). In section 4.6 we presented some of the effective interactions which can have impact on the Dirac fermions in graphene.

In the last part, we turned our sight to graphene nanoribbons. We took the Hamiltonian

(5.27) and interpreted it as a model of Dirac fermions in strained nanoribbon. We utilized the pre-prepared model from the section 3.2.1, especially the part (3.26). We figured out the energies of bound states for prescribed AC and ZZ b.c. We observed that strain had had different effects on AC and ZZ nanoribbons. Interestingly, the electrons in AC strained nanoribbons could be found with higher probability at the edges of nanoribbons, see Fig. 5.3. On the contrary, electrons in ZZ strained nanoribbons are located more in the middle of the nanoribbons, see Fig. 5.4. We identified the vector potential with the pseudo-magnetic field (5.26). The discussed 1D model can be understood as a subsystem of 2D setting with translation invariance. Our model has fixed value of longitudinal momentum $k_y = 0$. Since the momentum P_y is coupled with \tilde{A}_y and thus with k_y too, the DT will not help us in searching for the solution with arbitrary k_y . Extension of the results to genuinely 2D system is to be addressed in the future.

For the specific class of interactions, it is possible to assemble the 2D Dirac Hamiltonian from the 1D Dirac operator, see 5.6. It describes electrons in graphene without restrictions on k_y . We built a model of AC nanoribbon in the staggered field 5.7 which was based on the 1D solvable example 3.2.2. The band structures $E = E(k_y)$ of the model are depicted in Fig. 5.6. The results show that the application of an inhomogeneous staggered potential opens the band gap. Its width is smaller for the metallic AC nanoribbons than for the semiconducting ones. We revealed completely different behavior of density probability functions of electrons in various kinds of AC staggered nanoribbons, see Fig. 5.7. The model might find application in graphene electronics where the gap manipulations are important. But for that purpose the current available results on the topic should be analyzed carefully.



Bibliography

- [1] A. H. Castro Neto, F. Guinea, N. M. R. Peres, K. S. Novoselov, and A. K. Geim. The electronic properties of graphene. *Reviews of Modern Physics*, 81:109–162, 2009.
- [2] Mikhail I. Katsnelson. *Graphene: Carbon in Two Dimensions*. Cambridge University Press, 2012.
- [3] A. K. Geim and K. S. Novoselov. The rise of graphene. *Nature Mater*, 6:183–191, 2007.
- [4] Steven A. Vitale, Daniel Nezich, Joseph O. Varghese, Philip Kim, Nuh Gedik, Pablo Jarillo-Herrero, Di Xiao, and Mordechai Rothschild. Valleytronics: Opportunities, Challenges, and Paths Forward. *Small*, 14:1801483, 2018.
- [5] F. Guinea, M. I. Katsnelson, and A. K. Geim. Energy gaps and a zero-field quantum Hall effect in graphene by strain engineering. *Nature Physics*, 6:30–33, 2009.
- [6] Beibei Zhan, Chen Li, Jun Yang, Gareth Jenkins, Wei Huang, and Xiaochen Dong. Graphene Field-Effect Transistor and Its Application for Electronic Sensing. *Small*, 10:4042–4065, 2014.
- [7] T.O. Wehling, A.M. Black-Schaffer, and A.V. Balatsky. Dirac materials. *Advances in Physics*, 63:1–76, 2014.
- [8] F. Cooper, A. Khare, and U. P. Sukhatme. *Supersymmetry in Quantum Mechanics*. World Scientific Publishing Company Incorporated, 2001.
- [9] G. Junker. *Supersymmetric Methods in Quantum and Statistical Physics*. Springer Berlin, Heidelberg, 1 edition, 1996.
- [10] L.M. Nieto, A.A. Pecheritsin, and Boris F. Samsonov. Intertwining technique for the one-dimensional stationary Dirac equation. *Annals of Physics*, 305:151–189, 2003.

- [11] Wellisson Lima, Francisco Araújo, Diego Da Costa, S. Sena, and Joao Pereira. Tight-binding Model in First and Second Quantization for Band Structure Calculations. *Brazilian Journal of Physics*, 52, 2022.
- [12] Stephanie Reich, J. Maultzsch, Christian Thomsen, and P. Ordejón. Tight-binding description of graphene. *Phys. Rev. B*, 66:035412, 2002.
- [13] Mikhail I. Katsnelson. *Gauge fields and strain engineering*, page 243–265. Cambridge University Press, 2012.
- [14] Alonso Contreras-Astorga, Vít Jakubský, and Alfredo Raya. On the propagation of Dirac fermions in graphene with strain-induced inhomogeneous Fermi velocity. *Journal of Physics: Condensed Matter*, 32:295301, 2020.
- [15] A. R. Akhmerov and C. W. J. Beenakker. Boundary conditions for Dirac fermions on a terminated honeycomb lattice. *Physical Review B*, 77(8):085423, 2008.
- [16] L. Brey and H. A. Fertig. Electronic states of graphene nanoribbons studied with the Dirac equation. *Physical Review B*, 73, 2006.
- [17] Vít Jakubský, Şengul Kuru, and Javier Negro. Dirac fermions in armchair graphene nanoribbons trapped by electric quantum dots. *Physical Review B*, 105(16):165404, 2022.
- [18] Hermann Nicolai. Supersymmetry and spin systems. *Journal of Physics A: Mathematical and General*, 9:1497, 1976.
- [19] Edward Witten. Dynamical Breaking of Supersymmetry. *Nucl. Phys. B*, 188:513, 1981.
- [20] Gaston Darboux. Sur une proposition relative aux équations liéaires. *CR Acad. Sci. Paris*, 94:1456–1459, 1882.
- [21] Bogdan Mielnik and Oscar Rosas-Ortiz. Factorization: little or great algorithm? *Journal of Physics A: Mathematical and General*, 37:10007, 2004.
- [22] A. Zyablovsky, A. Vinogradov, A. Pukhov, Alexander Dorofeenko, and Alexander Lisyansky. PT-symmetry in optics. *Physics-Uspekhi*, 57:1063–1082, 2014.
- [23] Jim Lambers. Properties of Sturm-Liouville Eigenfunctions and Eigenvalues, 2016. <https://www.math.usm.edu/lambers/mat606/lecture20.pdf>.
- [24] Jingwei Jiang and Steven G. Louie. Topology Classification using Chiral Symmetry and Spin Correlations in Graphene Nanoribbons. *Nano Letters*, 21:197–202, 2021. PMID: 33320677.
- [25] G. Grosso and G. Pastori Parravicini. *Solid state physics*. Academic Press, 2014.
- [26] Sajedeheh Manzeli, Dmitry Ovchinnikov, Diego Pasquier, Oleg V. Yazyev, and Andras Kis. 2D transition metal dichalcogenides. *Nature Reviews Materials*, 2:17033, 2017.
- [27] Vít Jakubský. Spectrally isomorphic Dirac systems: Graphene in an electromagnetic field. *Physical Review D*, 91, 2015.

- [28] Xu Zhou, Qingyan Deng, Wentao Yu, Kaihui Liu, and Zhongfan Liu. The Rise of Graphene Photonic Crystal Fibers. *Advanced Functional Materials*, 32:2202282, 2022.
- [29] Kunze Lu, Manlin Luo, Weibo Gao, Qi Wang, Hao Sun, and Donguk Nam. Strong second-harmonic generation by sublattice polarization in non-uniformly strained monolayer graphene. *Nature Communications*, 14:2580, 2023.
- [30] Hela Ladjimi and Michał Tomza. Diatomic molecules of alkali-metal and alkaline-earth-metal atoms: interaction potentials, dipole moments, and polarizabilities. <https://doi.org/10.48550/arXiv.2303.17527>, 2023.